chemosensors

Review

Sensing Mechanisms of GPCR- and OBP-Based Biosensors for Addictive Drug Detection

Li Sin Wong [1], Xiaojing Zhang [1], Yanran Xia [1], Xinrui Tang [1], Hongyang Guo [1], Hongjian Zhang [2], Ping Wang [1,3,4], Boyang Xu [2,*] and Liujing Zhuang [1,3,*]

[1] Biosensor National Special Laboratory, Key Laboratory for Biomedical Engineering of Education Ministry, Zhejiang Key Laboratory of Intelligent Sensing Technology and Advanced Medical Instrument and Key Laboratory for Biomedical Engineering of Ministry of Education, College of Biomedical Engineering & Instrument Science, Zhejiang University, Hangzhou 310027, China; 22415084@zju.edu.cn (L.S.W.)
[2] Zhejiang Key Laboratory of Drug Prevention and Control Technology, National Narcotics Laboratory Zhejiang Regional Center, Hangzhou 310052, China
[3] The MOE Frontier Science Center for Brain Science & Brain-Machine Integration, The State Key Lab of Brain-Machine Intelligence, Zhejiang University, Hangzhou 310027, China
[4] Cancer Center, Binjiang Institute of Zhejiang University, Hangzhou 310027, China
* Correspondence: xbyxby2012@163.com (B.X.); zhuangliujing@zju.edu.cn (L.Z.)

Abstract

Addictive drug abuse remains a major global public health concern, creating a need for rapid and reliable approaches for drug screening and on-site analysis. Conventional analytical techniques provide accurate chemical identification but generally require laboratory-based instrumentation and sample processing. Biomimetic sensors incorporating biological recognition elements offer an alternative approach by exploiting molecular recognition and, in some cases, receptor-mediated signaling. This review summarizes recent progress in the use of G-protein-coupled receptors (GPCRs) and odorant-binding proteins (OBPs) as recognition elements for addictive drug-related sensing. The structural basis of ligand recognition and the native signaling mechanisms of GPCRs and OBPs are discussed, together with structural and computational studies that provide insight into drug-recognition element interactions. Recent sensing strategies based on electrical, optical, electrochemical, and acoustic transduction are then examined in terms of recognition mechanism, analytical performance, and application characteristics. Reported systems include direct measurements of drug–protein interactions, as well as functional assays that monitor receptor activation and downstream signaling. These studies demonstrate the potential of GPCR- and OBP-based recognition elements for sensitive detection of addictive drugs and related ligands, but also reveal limitations in discriminating structurally related compounds. In particular, receptor activation or ligand binding does not necessarily provide definitive chemical identification, which limits the direct application of activity-based sensing to forensic and regulatory analysis. Other challenges include maintaining functional recognition elements following immobilization, achieving reproducible coupling between molecular recognition and signal generation, and establishing performance in complex samples. Future development will require improved control of recognition-element interfaces, broader use of multiplexed recognition, and complementary analytical confirmation to improve the reliability and practical applicability of biomimetic sensors for addictive drug detection.

Keywords: addictive drug detection; G-protein-coupled receptors; biological recognition elements; biosensors; biomimetic sensors

Check for updates

Received: 6 August 2026
Revised: 21 September 2026
Accepted: 1 October 2026
Published: 8 October 2026

Copyright: © 2026 by the authors. Licensee MDPI, Basel, Switzerland. This article is an open access article distributed under the terms and conditions of the Creative Commons Attribution (CC BY) license.

1. Introduction

The abuse of addictive drugs, whether traditional opioids such as heroin and morphine, new synthetic drugs such as methamphetamine (METH) and fentanyl, or even certain abused prescription medications, has become a severe global public health issue [1–3]. These substances not only inflict devastating damage on individual physical and mental health, leading to neurological disorders, organ failure, psychiatric conditions and even death, but also trigger a series of profound social problems including family breakdown, violent crime, and disease transmission [1–3]. Therefore, developing technologies capable of detecting addictive drugs in a rapid, sensitive, specific and portable manner is of critical practical significance for clinical toxicological diagnosis, forensic investigations, drug law enforcement, and drug abuse monitoring and early warning.

Conventional techniques such as gas chromatography–mass spectrometry (GC-MS) and liquid chromatography–mass spectrometry (LC-MS) remain widely used reference or confirmatory methods for the identification and quantification of addictive drugs, by virtue of their sensitivity, specificity and the extensive spectral libraries available. Their reliance on costly instrumentation, demanding operation, laborious sample pretreatment and protracted analysis times [4,5] nevertheless render them ill-suited to on-site testing and large-scale screening. Immunoassay platforms such as the enzyme-linked immunosorbent assay (ELISA) are by contrast simple, high-throughput and inexpensive, and are widely deployed for the preliminary screening of large sample cohorts; yet, antibody-based recognition can result in cross-reactivity and limited availability of antibodies for emerging psychoactive substances [6], such that the results obtained are generally presumptive and often class-level, requiring confirmatory analysis by LC-MS. Capillary electrophoresis (CE) provides high separation efficiency, low sample consumption, and compatibility with multiple detection modes, but its sensitivity and reproducibility can be affected by limited sample loading and strict control of separation conditions [7]. Fourier-transform infrared (FTIR) spectroscopy enables rapid, largely non-destructive fingerprinting with minimal sample pretreatment and is increasingly used for preliminary screening, including in field settings, although its sensitivity is limited for minor constituents and its performance depends on spectral libraries [8].

Field-deployable techniques generally trade a measure of analytical rigour for speed, portability and ease of use. Lateral flow immunoassays (LFIAs) and point-of-care immunoassay readers extend the antibody-based recognition underpinning ELISA to disposable formats that dispense with bench-scale instrumentation, and are well suited to roadside checks, workplace screening and the on-scene testing of urine or oral fluid by law enforcement [9,10]; sensitivity is nonetheless modest, and the limitations associated with cross-reactivity persist. Ion mobility spectrometry (IMS) and laser-induced breakdown spectroscopy (LIBS), founded respectively on gas-phase ion mobility and laser-induced atomic emission, provide near-real-time, non-immunological alternatives with favourable portability and response times. IMS is, however, constrained by matrix and background interference and by insufficient resolving power [11], whereas the information furnished by LIBS is largely elemental rather than molecular [12]; both are therefore employed chiefly for preliminary triage or for the characterisation of adulterants rather than for definitive drug identification. Raman spectroscopy affords molecularly specific, non-destructive fingerprinting and permits analysis through transparent packaging, but the weakness of the scattered signal and its susceptibility to background interference from the sample or its packaging curtail its utility for trace-level or heavily adulterated samples [13]. A comparison of representative conventional and field-deployable approaches is summarized in Table 1. Collectively, these methods highlight a persistent trade-off between analytical performance and operational accessibility, particularly in terms of specificity, sensitivity, speed,

and portability. Consequently, the construction of highly selective biosensors has become one of the important directions for the rapid and sensitive detection of addictive drugs.

Unlike antibodies or enzymes traditionally employed in biosensing, G-protein-coupled receptors (GPCRs) and odorant-binding proteins (OBPs) provide biologically derived molecular recognition elements with the ability to interact selectively with diverse small molecules. GPCRs can recognize extracellular chemical signals and convert ligand binding into receptor conformational changes and downstream signaling events, whereas soluble OBPs bind odorant and other small molecules through defined ligand-binding pockets [14,15]. These characteristics have motivated the incorporation of GPCRs and OBPs into biomimetic sensing platforms, where ligand-recognition events can be coupled with physical or biological transduction mechanisms to generate measurable analytical signals.

This review focuses on the use of GPCRs and OBPs as biomimetic recognition elements for addictive drug-related sensing, rather than on conventional analytical detection methods alone. Three related but distinct research directions are considered: direct detection of addictive drug molecules, monitoring of receptor activation induced by drug–receptor interactions, and investigation of endogenous ligands involved in related signaling pathways. Although several GPCRs and OBPs have been explored as recognition elements for chemically diverse compounds, their application to addictive drug-related sensing remains relatively limited. Within the scope of the literature examined in this review, sensing studies have been reported for cannabinoid receptors, opioid receptors, and OBPs, whereas corresponding sensing applications involving mammalian olfactory receptors (ORs) and trace amine-associated receptors (TAARs) have not yet been identified. This limited representation of OR- and TAAR-based sensing highlights the relatively early stage of research at the intersection of these recognition systems and addictive drug detection. Accordingly, this review summarizes the molecular recognition mechanisms and signal transduction strategies underlying GPCR- and OBP-based sensing, while critically discussing the current limitations and future research opportunities in this emerging field.

Relevant literature was primarily identified through searches of the Web of Science database using combinations of keywords related to GPCRs, OBPs, biosensors, biomimetic sensing, and addictive drugs. Additional relevant studies were identified through reference-list examination and citation tracking to provide a broader overview of the available literature.

Table 1. Comparison of representative laboratory-based and on-site point-of-care methods for the detection of addictive drugs.

Method	Principle	Advantages	Limitations
GC-MS [4]	Gas chromatographic separation followed by mass-spectral identification and quantification.	High sensitivity and specificity; excellent discrimination of structurally similar drugs; quantitative analysis; extensive spectral libraries.	Requires volatile or derivatized analytes; complex pretreatment for polar or thermally labile compounds; expensive and bulky instrumentation; trained personnel required.
LC-MS [5]	Liquid chromatographic separation followed by ESI/APCI-MS detection and quantification.	Broad analyte coverage; high sensitivity and selectivity; suitable for polar, non-volatile, and thermally labile compounds.	High acquisition and operating costs; complex pretreatment; matrix effects and ion suppression; relatively long analysis workflow; skilled operation required.

Table 1. *Cont.*

Method	Principle	Advantages	Limitations
ELISA [6]	Antigen–antibody recognition in competitive or non-competitive formats, with enzymatic, fluorescent, or chemiluminescent signal generation.	High throughput; relatively low cost; applicable to urine, blood, saliva, and hair; suitable for preliminary screening.	Cross-reactivity with structurally related compounds; presumptive and often class-level results; limited antibody availability for emerging psychoactive substances.
CE [7]	Electrophoretic separation of charged analytes according to differences in migration mobility, coupled with UV, LIF, or MS detection.	High separation efficiency and resolution; very low sample consumption; relatively low operating cost; compatible with multiple detection modes.	Sensitivity may be limited for trace-level drugs; reproducibility depends on precise control of separation conditions.
FTIR [8]	Identification based on characteristic molecular vibrational absorption fingerprints and comparison with reference spectra.	Rapid; largely non-destructive; applicable to solid, liquid, and gaseous samples; minimal pretreatment; portable instruments available.	Relatively low sensitivity; library-dependent; spectral overlap complicates analysis of mixtures; strongly colored or opaque samples may interfere with measurements.
LFIA [9]	Capillary migration of the sample through a membrane, followed by competitive or sandwich immunoreaction and visual or optical signal readout.	Simple and rapid; low cost; suitable for non-specialists and on-site testing of urine or oral fluid.	Limited sensitivity and quantitative capability without signal enhancement; hook effect at high analyte concentrations; class-level rather than compound-specific detection; cross-reactivity.
POCT immunoassay reader [10]	Portable reading of colorimetric, fluorescent, or electrochemical signals generated by LFIA or cartridge-based immunoassays.	Rapid; simple operation; portable; suitable for decentralized testing.	Limited analytical reliability in some applications; false-positive and false-negative results may occur; performance depends on assay-specific cutoff settings.
IMS [11]	Ionization of trace vapors or particles followed by gas-phase separation according to ion mobility in an electric field.	Rapid analysis; portable and robust instrumentation; good sensitivity for multiple drug classes.	Susceptible to matrix/background interference and competitive ionization; peak overlap may cause false alarms; reduced resolving power for complex samples; GC coupling may be required.
LIBS [12]	Laser-induced ablation generates plasma, and characteristic atomic/ionic emission spectra are recorded for elemental analysis.	Rapid; minimal sampling; little or no pretreatment; applicable to solids, liquids, and gases; non-contact or remote analysis possible.	Primarily provides elemental rather than molecular information; cannot directly confirm specific organic drug compounds; strongly dependent on matrix and instrumental conditions.
Raman spectroscopy [13]	Molecular identification based on characteristic vibrational fingerprints generated by inelastic light scattering.	Rapid and non-destructive; minimal pretreatment; analysis through transparent packaging; portable instruments available.	Weak intrinsic Raman scattering; fluorescence from samples or packaging may obscure signals; limited sensitivity for low-concentration analytes; challenging analysis of complex mixtures.

2. Structural and Signal Transduction Basis of Endogenous Biorecognition Elements for Addictive Drug Detection

In the chemical sensing systems of mammals and insects, GPCRs and OBPs constitute core functional units. In the mammalian nervous system, GPCRs such as cannabinoid receptors, opioid receptors, and TAARs can recognize endogenous signaling molecules as well as exogenous psychoactive compounds, including addictive drugs [16,17] (Figure 1). Ligand binding to these receptors is mediated by interactions within defined binding pockets and can induce receptor conformational changes and subsequent intracellular signaling events [17–19]. In contrast, OBPs are soluble proteins involved in the binding, transport, and presentation of hydrophobic small molecules in olfactory systems [20,21]. Their ligand-binding cavities accommodate structurally diverse odorant molecules and contribute to odorant recognition in complex chemical environments [22,23]. Although GPCRs and OBPs differ in structure, localization, and biological function, both possess defined ligand-binding sites that mediate selective interactions with small molecules. Their structural characteristics, ligand-binding modes, and native signaling mechanisms are therefore relevant to the development of biomimetic sensing strategies.

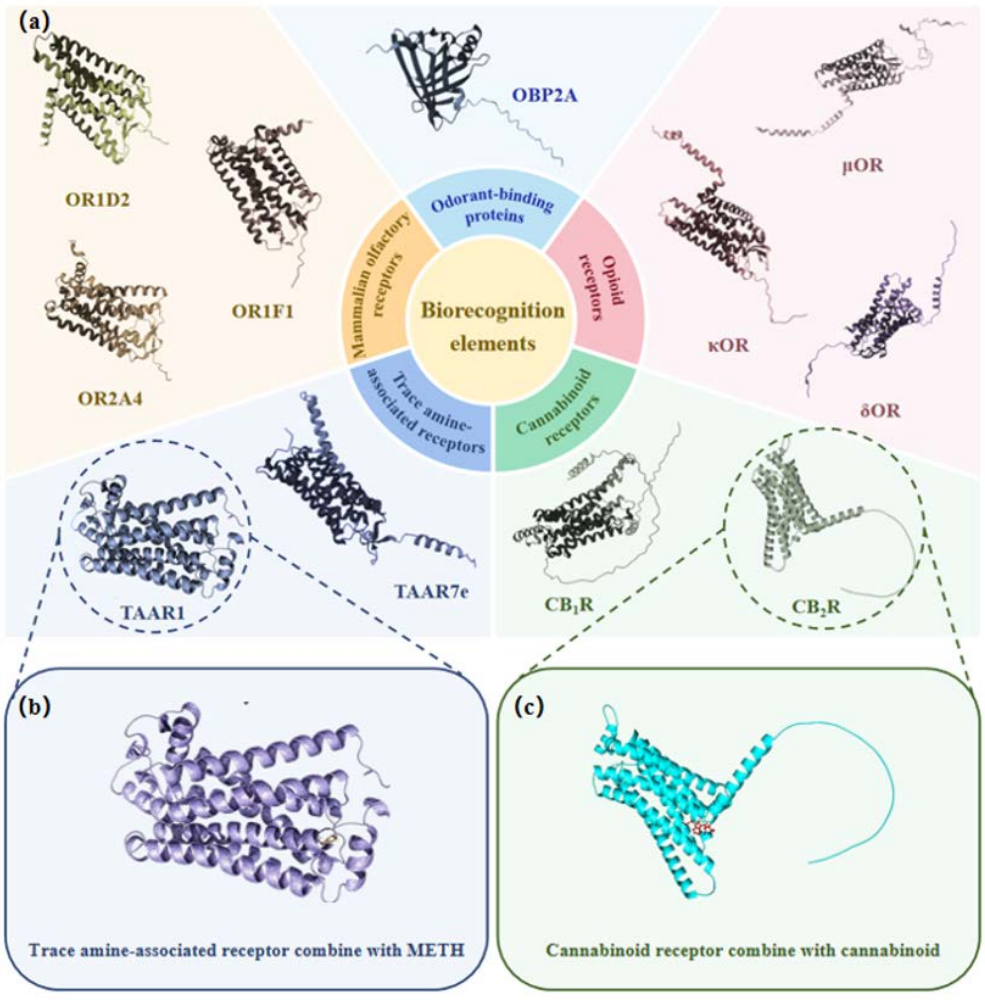


Figure 1. (**a**) Schematic of endogenous biorecognition elements for addictive drugs; (**b**) TAAR1 bound to METH; (**c**) CB_2R combined with cannabinoid.

GPCRs are a class of membrane receptor proteins widely distributed in cells and play a crucial role in cell signal transduction. GPCRs are composed of a single polypeptide chain and generally possess seven transmembrane α-helical domains [24]. This unique

structure enables them to interact simultaneously with extracellular signaling molecules and intracellular G proteins [25]. G proteins are heterotrimeric complexes composed of α, β, and γ subunits (Gαβγ), with the Gα subunit being divided into subtypes like $G\alpha_q$, $G\alpha_s$, $G\alpha_i$, and $G\alpha_o$ [26]. In the inactive state, Gα binds guanosine diphosphate (GDP), keeping the G protein in an inactive conformation with the three subunits tightly associated. This inactive G protein is typically coupled to the corresponding unactivated GPCRs and is located on the inner side of the cell membrane. Upon ligand binding, GPCRs undergo a conformational change that activates the corresponding G protein signaling pathway. At this point, GDP on Gα is replaced by guanosine triphosphate (GTP), leading to the release of Gα-GTP and Gβγ. The dissociated Gα-GTP complex and Gβγ can act as signaling molecules to further activate downstream effectors inside the cell [26].

When the $G\alpha_q$ signaling pathway is activated, the ligand-bound GPCR activates $G\alpha_q$, which in turn activates phospholipase Cβ (PLCβ) [27], generating diacylglycerol (DAG) and inositol 1,4,5-trisphosphate (IP3). DAG activates protein kinase C (PKC), which participates in processes such as inflammatory responses [27], whereas IP3 binds to intracellular IP3 receptors, raising cytosolic calcium (Ca^{2+}) levels [27] and thereby activating calcium/calmodulin-dependent protein kinase II (CaMKII), which has shown ameliorative effects in schizophrenia models [28]. In contrast, $G\alpha_i$ generally mediates signaling downstream of stimulatory GPCRs. Upon activation of the $G\alpha_i$ signaling pathway, $G\alpha_i$-GTP inhibits adenylyl cyclase (AC), reducing intracellular cyclic adenosine monophosphate (cAMP) levels and consequently attenuating protein kinase A (PKA) activity, directly modulating ion channel function [29]. In contrast, the $G\alpha_s$ signaling pathway operates in the opposite manner: $G\alpha_s$ as a stimulatory G protein, generally mediates signaling downstream of stimulatory GPCR activation. When the $G\alpha_s$ pathway is activated, $G\alpha_s$-GTP activates AC to elevate intracellular cAMP levels, which in turn activates PKA to participate in regulating cellular functions and is related to the efficacy of antipsychotic drugs [28]. Gβγ activates G protein-coupled inwardly rectifying potassium channels (GIRK), promoting potassium ion (K^+) efflux and inducing neuronal hyperpolarization [29,30], while simultaneously inhibiting voltage-gated calcium channels (VGCCs), reducing Ca^{2+} influx and neurotransmitter release, ultimately suppressing neuronal excitability and mediating analgesic effects [29]. The GTPase activity of Gα hydrolyzes GTP, after which Gα-GDP reassociates with Gβγ to form inactive Gαβγ, terminating the signal [26,29].

2.1. Cannabinoid Receptors

Cannabinoid receptors belong to class A GPCRs and primarily comprise two subtypes: cannabinoid receptor 1 (CB_1R) and cannabinoid receptor 2 (CB_2R) [31,32]. CB_1R is highly enriched in the central nervous system, with particularly high expression in regions such as the hippocampus and cerebral cortex [31,32], and is the most highly expressed GPCR in the human brain [33,34]. CB_1R participates in regulating physiological activities including neurotransmitter release, reward circuitry, pain perception, and cognitive functions [31,32,35]. By contrast, CB_2R is mainly located in the peripheral immune system, including glial cells and lymphocytes [31,32], and has a critical function in neuroinflammation and immune regulation [32,35]. Although CB_1R and CB_2R share approximately 44% overall sequence identity and approximately 68% sequence similarity within their transmembrane regions [36], they exhibit distinct ligand-recognition and signaling properties. CB_1R primarily signals through coupling to $G\alpha_i$, mediating the AC-cAMP-PKA pathway [29,30]. Owing to hydrophobic interactions of key residues in the extracellular loops, CB_1R can also couple to $G\alpha_s$ and $G\alpha_q$ under specific conditions [29,30]. In CB_2R, the action of specific residues in its extracellular loops restricts its primary coupling to $G\alpha_i$, thereby inhibiting the AC-cAMP-PKA pathway [29,30].

As an example, synthetic cannabinoids are a class of artificially synthesized new psychoactive substances that exhibit pharmacological effects similar to those of tetrahydrocannabinol (THC) [37]. Unlike traditional addictive drugs, whose chemical structures are relatively stable, synthetic cannabinoids can undergo extensive structural diversification through the substitution of four key pharmacophoric groups: the core scaffold, the linker group, the head group, and the tail group [38]. By modular replacement, modification, or rearrangement, illicit manufacturers can generate novel variants designed to circumvent existing legal regulations while maintaining or even enhancing receptor affinity [38]. For such structurally diverse substances, cannabinoid receptor-based detection methods do not rely solely on recognition of specific molecular structures but instead monitor receptor activation induced by ligand binding. This mechanism may allow receptor-based sensors to respond to newly emerging synthetic cannabinoids with diverse chemical structures, provided that the compounds retain sufficient receptor activity and generate a measurable sensor response.

In 2016, Hua et al. [34] determined the crystal structure of CB_1R in complex with the antagonist AM6538, elucidating the ligand-recognition mechanism of CB_1R at the atomic level. Radioligand binding assays demonstrated that AM6538 exhibits strong binding affinity and wash resistance toward wild-type CB_1R, indicating an extremely slow dissociation rate, which is favorable for stabilizing the receptor conformation and promoting crystallization. Structural analysis revealed that the N-terminus of CB_1R forms a V-shaped loop that inserts into the binding pocket, restricting ligand access, and that multiple residues in extracellular loop 2 extend into the binding pocket and are crucial for ligand recognition. Molecular docking accurately reproduced the embedding of the three functional arms of AM6538 into three sub-pockets formed by the transmembrane helices (TM), extracellular loop 2, and the N-terminus, respectively, validating the structural basis for its multi-point cooperative stabilization of binding. Quantum mechanical calculations further confirmed that the conformation of AM6538 in the crystal is close to a local energy minimum, verifying the rationality of the binding conformation. Site-directed mutagenesis of key residues showed that the antagonistic potency of AM6538 was significantly reduced upon mutation, suggesting that these residues contribute to AM6538 binding through π-π interactions. In addition, molecular docking predicted the binding modes of agonists such as THC, anandamide (AEA), 2-arachidonoylglycerol (2-AG), and the synthetic cannabinoid JWH-018. It was found that the phenol ring of THC forms π-π bonds with aromatic residues and its pentyl side chain inserts into a hydrophobic channel; the alkyl chains of AEA and 2-AG likewise insert into hydrophobic channels formed by the TM; and the naphthalene ring of JWH-018 engages in π-π stacking interactions with aromatic residues. The binding pockets of agonists and antagonists partially overlap but display key conformational differences, providing a structural basis for differences in ligand recognition and receptor activation among cannabinoid ligands. This study provides structural insights for developing CB_1R-targeting anti-addiction drugs and CB_1R-based biomimetic sensing platforms.

2.2. Opioid Receptors

Opioid receptors also belong to the GPCR family, comprising subtypes including the μ-opioid receptor (μOR), δ-opioid receptor (δOR), and κ-opioid receptor (κOR) [39]. They are highly expressed in regions such as the dorsal horn of the spinal cord and the thalamus [40,41] and are involved in regulating pain transmission, emotional responses, and reward circuitry [42]. Opioid receptors are the primary targets of endogenous opioid peptides, such as endorphins and enkephalins, as well as exogenous opioid drugs, such as fentanyl and morphine [39]. Dysfunction of these receptors is closely associated with pain disorders, drug addiction, and respiratory depression [39]. Opioid receptors mainly act

through the $G\alpha_i$-mediated AC-cAMP-PKA signaling pathway [43]. Through this pathway, they inhibit neuronal activity in the respiratory center [44], reduce the sensitivity of the respiratory center to carbon dioxide [45], leading to a marked decrease in respiratory rate and depth, which is the primary cause of death from opioid overdose.

In 2022, Zhuang et al. [46] first resolved the high-resolution structures of the human μOR in complex with G protein and ligands such as fentanyl and morphine using cryo-electron microscopy (cryo-EM). The study revealed that fentanyl and morphine, both opioid drugs, display markedly different binding modes within the μOR orthosteric binding pocket. Fentanyl adopts a "Y"-shaped conformation: its phenethyl group inserts into a hydrophobic subpocket between TM2/3, interacting with residues such as glutamine, whereas its N-aniline ring forms π-π stacking interactions with tryptophan and tyrosine residues in the TM6/7 region. In contrast, morphine adopts a compact "O"-shaped conformation, capable only of forming a salt bridge and hydrophobic interactions with key residues, and fails to occupy the TM2/3 subpocket unique to fentanyl, which may contribute to the markedly higher agonistic potency of fentanyl compared to morphine. Site-directed mutagenesis and molecular dynamics simulations further demonstrated that tryptophan and other residues in the TM6/7 region exert only a modest influence on cAMP inhibition induced by fentanyl and morphine, rather than being major determinants of G protein-mediated signaling. Based on this mechanism, the research team designed fentanyl analogs FBD1 and FBD3. By reducing the size of the N-aniline group to weaken TM6/7 interactions, they successfully obtained compounds that retain G protein activity and exhibit biased signaling toward the G protein pathway, providing a feasible strategy for designing novel μOR agonists. This study provides structural insights into the structure–activity relationships of opioid ligands and their interactions with μOR.

2.3. Trace Amine-Associated Receptors (TAARs)

The trace amine-associated receptor family belongs to the rhodopsin-like class A GPCRs [47] and contains multiple members [47]. Among them, trace amine-associated receptor 1 (TAAR1) is one of the more extensively studied members. TAAR1 is widely distributed in the brain [47] and has particularly high expression in the dopamine (DA) ventral tegmental area (VTA) and other regions [48]. It participates in regulating physiological processes such as reward circuitry and emotional states [48] and is associated with the pathogenesis of schizophrenia, depression, and drug addiction [48–50]. TAAR1 can specifically recognize and bind various biogenic amines, interacting with endogenous trace amines such as β-phenylethylamine (β-PEA) and tryptamine, as well as exogenous substances such as amphetamine, METH (methamphetamine), and 3,4-methylenedioxymethamphetamine (MDMA) [48], and couples with different G protein subtypes such as $G\alpha_q$, $G\alpha_s$, and $G\alpha_i$, mediating diverse biological effects [28].

In 2023, Liu et al. [51] used cryo-electron microscopy (cryo-EM) to determine the first high-resolution structures of the TAAR1-$G\alpha_s$ complex bound to METH and β-PEA, revealing the activation mechanism of TAAR1 at the atomic level. The study found that the amino group of METH forms a salt bridge with a conserved aspartate residue in the orthosteric pocket of TAAR1, and is stabilized by a hydrogen-bond network composed of tyrosine, serine, and other residues, while its phenylpropyl moiety engages in hydrophobic interactions with multiple hydrophobic residues. Mutagenesis experiments confirmed that mutation of the conserved aspartate or tyrosine almost completely abolished METH-induced receptor activation, validating that the salt bridge and hydrogen-bond network are critical for TAAR1 activation by METH; mutations of serine and several hydrophobic residues also markedly reduced agonist potency, indicating that polar interactions and hydrophobic contacts together govern the high-affinity binding and receptor activation of

METH. Although β-PEA shares a similar binding mode with METH, its amino group forms shorter hydrogen bonds with the aspartate and serine, and the tyrosine directly engages β-PEA, which may contribute to the more than 10-fold higher activation efficacy of β-PEA compared with METH. Upon binding to TAAR1, METH promotes $G\alpha_s$ coupling and cAMP accumulation. Furthermore, molecular dynamics simulations showed that METH exhibits greater binding stability in the rodent TAAR1 pocket than in the human receptor, which may contribute to species-dependent differences in TAAR1 pharmacology. Hydrophobic residues on extracellular loop 2 (ECL2) of TAAR1 restrict the pocket volume, making it better suited for small trace amine molecules, whereas differences in these key residues among TAAR family members may contribute to their distinct responses to ligands such as METH. This study elucidates the structural basis of TAAR1 recognition and activation by diverse amine ligands at the atomic level.

2.4. Mammalian Olfactory Receptors (ORs)

Mammalian ORs belong to the class A GPCR superfamily [52] and represent one of the largest multigene families in vertebrate genomes [53]. In humans, there are approximately 400 functional ORs [53], whereas in mice the number exceeds 1000 [54]. Mammalian ORs are characterized by substantial sequence diversity and ligand specificity, and their evolutionary trajectory is closely linked to environmental adaptation and an enhanced capacity to process complex olfactory information [53,55]. ORs are primarily expressed on the dendrites of olfactory sensory neurons located in the main olfactory epithelium within the nasal cavity [52]. A single olfactory sensory neuron typically expresses one OR gene [56], ensuring the specific transmission of olfactory information. By specifically recognizing volatile odorant molecules in the environment [52], mammalian ORs convert chemical signals into neural electrical signals [57], allowing for the discrimination and identification of diverse odorants and thereby enabling complex olfactory perception and behavioral responses.

Signal transduction of mammalian ORs principally relies on the olfactory neuron-specific Gα ($G\alpha_{olf}$) pathway [57], in which $G\alpha_{olf}$ shares 88% sequence identity with $G\alpha_s$. Upon odorant binding, the conformational change in the OR promotes GDP-GTP exchange on $G\alpha_{olf}$. The dissociated $G\alpha_{olf}$-GTP specifically activates adenylyl cyclase III (ACIII) [58], leading to an increase in cAMP concentration that directly acts on cyclic nucleotide-gated (CNG) ion channels. This induces Na^+ and Ca^{2+} influx, resulting in depolarization of the olfactory sensory neuron [57,58]. The incoming Ca^{2+} further activates calcium-activated chloride channels (CaCCs), which amplify the depolarization via chloride efflux, ultimately triggering action potentials that are transmitted to the olfactory bulb [57]. Consequently, the olfactory signals are relayed to the olfactory centers of the brain for further processing and recognition. Meanwhile, cAMP is hydrolyzed and degraded by phosphodiesterase (PDE), and $G\alpha_{olf}$ hydrolyzes GTP through its intrinsic GTPase activity, allowing $G\alpha_{olf}$ and $G\beta\gamma$ subunits to reassociate into an inactive state, thereby completing the signaling cycle [58].

In 2015, Ho et al. [59] investigated the interaction of ketamine with mouse ORs and elucidated the molecular mechanism by which ketamine selectively recognizes and activates specific ORs. The study found that among 51 mouse ORs, only MOR136-1, MOR136-3, and MOR139-1 exhibited concentration-dependent activation by ketamine, with half-maximal effective concentration (EC_{50}) values close to the plasma ketamine levels observed under anesthesia in mice. Homology modeling and molecular docking identified a ketamine-binding pocket composed primarily of 16 residues from TM3/5/6, among which key residues such as serine and aspartate stabilize the protonated secondary amine and the ketone group (C=O) of ketamine through hydrogen-bonding and electrostatic interactions.

Site-directed mutagenesis confirmed that mutation of specific residues in the responsive receptor MOR136-1 could eliminate or enhance the response to ketamine, whereas mutation of residues in the non-responsive receptor MOR136-4 conferred ketamine sensitivity stronger than that of the wild-type, supporting the functional importance of these residues in ketamine recognition and receptor activation. In vivo in situ hybridization and pS6 staining demonstrated that intranasal administration of ketamine dose-dependently activated olfactory sensory neurons expressing MOR136-1, indicating that olfactory receptors can serve as functional targets of ketamine in a physiological environment. This study provides evidence for novel G protein-coupled receptor targets underlying the anesthetic, analgesic, and antidepressant effects of ketamine.

2.5. Odorant-Binding Proteins

OBPs are important soluble carrier proteins in the olfactory systems of mammals and insects, responsible for transporting odorant molecules in the aqueous environment [60]. Mammalian OBPs belong to the lipocalin superfamily and are mainly found in biological fluids such as nasal mucus, urine, and saliva [61]. They possess a typical β-barrel structure composed of eight antiparallel β-strands and a short C-terminal α-helix, which forms an internal hydrophobic binding cavity for accommodating small hydrophobic molecules [61]. In contrast, insect OBPs are small secretory proteins highly expressed in the sensillar lymph of olfactory organs such as antennae and mouthparts. They generally feature an N-terminal signal peptide, and their typical structure is predominantly α-helical, forming a highly compact hydrophobic binding cavity through three disulfide bonds [62]. Insect OBPs can be classified into various subtypes based on the number of cysteine residues and sequence characteristics, and they exhibit different binding affinities and selectivities for different classes of odorant molecules [22]. These properties are considered to contribute to the precise recognition of complex odor environments by insects [22,63].

In the olfactory system, OBPs act as transport carriers for odorant molecules. Through hydrophobic interactions, van der Waals forces, and hydrogen bonds, they specifically bind and solubilize hydrophobic or amphiphilic odorants from the environment, overcoming solubility limitations in aqueous surroundings and diffusing stably in aqueous mucus or sensillar lymph [22], thereby facilitating their transport through the aqueous environment [63]. When the OBP-odorant complex diffuses to the dendritic membrane surface of olfactory sensory neurons, the odorant molecule is released from the OBP and subsequently recognized and bound by neighboring ORs, activating olfactory signal transduction and triggering an olfactory response [61]. However, the precise mechanism by which OBPs release odorants and activate ORs remains subject to different hypotheses and unresolved questions [64]. OBPs are also thought to rebind and carry away odorant molecules from the vicinity of ORs after activation, working together with metabolic enzymes to clear the odorants, thereby terminating the olfactory signal and preventing adaptation or receptor saturation caused by continuous stimulation [61,64].

In 2018, Langeswaran et al. [65] systematically revealed the molecular mechanisms by which honeybee OBPs efficiently recognize illicit drugs and explosives, providing a theoretical basis for the development of OBP-based biosensing technology and the use of live honeybees for on-site detection. The study integrated 43 honeybee OBPs with 19 compounds, including cocaine, methadone, dronabinol, and MDMA, and found that specific OBPs showed favorable docking scores with several addictive drug molecules. Notably, several drug–OBP complexes exhibited favorable docking scores, including crack cocaine with 3BJH (−11.75 kcal/mol), methadone with OBP10 (−11.71 kcal/mol), dronabinol with 1TUJ (−11.66 kcal/mol), and MDMA with OBP24 (−10.89 kcal/mol), suggesting potential binding preferences of these OBPs toward addictive drugs, although further experimental

validation is required to confirm their binding affinity and selectivity. Furthermore, the study elucidated the molecular interactions between OBPs and addictive drugs, showing that addictive drugs containing amino groups, such as amphetamine, bind via hydrogen bonds to negatively charged residues like aspartate in the active cavity of OBPs, whereas addictive drugs with aromatic ring structures, such as methadone, rely on π-π stacking interactions with hydrophobic residues like tryptophan and phenylalanine. Density functional theory (DFT) calculations showed that compounds with favorable docking scores were also associated with lower HOMO–LUMO gaps in the reported DFT analysis. The HOMO orbitals were mainly localized on aromatic rings or amino-containing regions, whereas the LUMO distributions highlighted electron-accepting regions. These calculations provided additional information on the electronic structures of the drug molecules that may help interpret their interactions with OBPs. Based on these results, the study proposed a dual-application strategy: compounds with favorable binding preferences could potentially be targeted through trained live honeybees for on-site detection, whereas OBP-based molecular biosensors could be developed for compounds showing favorable interactions in the computational analysis. This work elucidated the molecular basis of interactions between honeybee OBPs and addictive drugs and explosives at the computational level and provided information for exploring OBP-based biosensing in security screening and related applications.

The major GPCR and OBP recognition elements discussed above are summarized in Table 2, together with their representative ligands, signaling pathways, and relevance to addictive drug recognition.

Table 2. Comparison of endogenous biorecognition elements for addictive drug sensing.

Recognition Element	Molecular Class	Main Targets	Recognition/Signaling Mechanism	Advantages for Sensing	Limitations
CB_1R/CB_2R	GPCR	Cannabinoids	$G\alpha_i/G\alpha_s/G\alpha_q$	Ligand-induced receptor activation can be monitored	Subtype-dependent responses and structural diversity of cannabinoid ligands
μOR/δOR/κOR	GPCR	Opioids	$G\alpha_i$	High-affinity recognition of opioid ligands; functional responses can be monitored	Overlapping recognition profiles among structurally related opioids
TAAR1	GPCR	Amphetamine, METH, MDMA	$G\alpha_s/G\alpha_i/G\alpha_q$	Ligand-specific recognition of trace amines and stimulant ligands	Limited integration into addictive-drug sensing platforms
ORs	GPCR	Volatile psychoactive compounds	$G\alpha_{olf}$-cAMP pathway	Large receptor repertoire and ligand-specific responses	Limited application in addictive-drug detection
OBPs	Soluble binding proteins	Hydrophobic drugs	Ligand transport/binding	Soluble proteins compatible with surface immobilization	Ligand selectivity varies among OBPs; experimental validation remains limited

3. Immobilization Strategies for GPCR- and OBP-Based Recognition Elements

Stable immobilization of biorecognition elements such as GPCRs and OBPs onto sensor interfaces is an important step in the construction of biomimetic sensors. The immobilization strategy not only affects the interfacial stability of the recognition elements, but also influences their spatial orientation, accessibility of ligand-binding sites, and biological activity. For soluble OBPs, relatively straightforward surface immobilization approaches can generally be employed, whereas the transmembrane structure of GPCRs requires consideration of membrane dependence, the lipid microenvironment, and receptor conformation. Therefore, this section discusses physical adsorption, self-assembled monolayers (SAMs), covalent coupling, biotin–avidin/streptavidin immobilization, and histidine-tag (His Tag)/nitrilotriacetic acid (NTA) immobilization, with emphasis on their practical applications and key characteristics in GPCR- and OBP-based sensors.

3.1. Physical Adsorption

Physical adsorption is one of the simplest approaches for protein immobilization [66] and mainly relies on noncovalent interactions between proteins and solid surfaces, including electrostatic interactions, hydrophobic interactions, van der Waals forces, and hydrogen bonding [67,68]. Typically, a solution containing the target protein is brought into contact with the sensor surface and incubated to allow protein adsorption to occur, followed by buffer washing to remove unbound proteins [68]. This approach does not require additional chemical activation or protein pretreatment and offers advantages such as operational simplicity, mild conditions, and low cost [66]. It is therefore suitable for sensor prototyping and preliminary evaluation of the performance of recognition elements.

Physical adsorption has been applied to the construction of actual OBP- and GPCR-related interfaces. Zhao et al. [69] immobilized AaegOBP22 on a ZnO thin-film surface by physical adsorption and constructed an OBP-based acoustic sensor using a bulk acoustic wave resonator for the detection of small-molecule analytes such as N,N-diethyl-meta-toluamide (DEET). This study demonstrated that OBPs can be directly immobilized on inorganic surfaces through noncovalent interactions and used for target-molecule recognition without extensive chemical modification. Du et al. [70] used the olfactory receptor ODR-10 as a model receptor and employed physical adsorption as a control immobilization strategy in a quartz crystal microbalance (QCM) sensor to compare the effects of different immobilization approaches on OR-based sensing performance. Their results showed that physical adsorption can be used to construct an interface for GPCR-type olfactory receptors, although its sensing performance was lower than that achieved with specific immobilization strategies.

However, because physical adsorption relies on noncovalent interactions, its interfacial stability is generally lower than that of covalent immobilization, and protein desorption may occur in response to changes in buffer conditions, ionic strength, or complex sample environments [66,68]. In addition, the orientation of proteins adsorbed onto surfaces is generally difficult to control, and the accessibility of some recognition sites may be reduced when they face the surface [67]. For GPCRs, contact with a solid surface may affect receptor conformation and ligand binding; therefore, the lipid environment and membrane-mimicking structures should also be considered during immobilization to preserve receptor function [68].

3.2. Self-Assembled Monolayer (SAM)

SAMs are commonly used as a surface-engineering strategy for constructing functionalized sensing interfaces, particularly on noble-metal surfaces such as gold and silver.

Their basic principle involves the self-assembly of organic molecules with specific terminal groups on the gold surface, forming a relatively well-ordered molecular layer [71]. For example, alkanethiols can form self-assembled monolayers on gold through Au-S interactions, while their terminal groups can be functionalized with carboxyl, amino, biotin, or NTA groups for subsequent protein immobilization or specific capture [72,73]. Thus, SAMs are generally not an independent protein immobilization method, but rather serve as an intermediate layer for controlling the chemical properties of the protein-sensor interface.

SAMs have been applied to the construction of OBP- and GPCR-related sensing systems. Cali et al. [74,75] used thioctic acid to form a carboxyl-terminated SAM on a gold surface, followed by 1-ethyl-3-(3-dimethylaminopropyl) carbodiimide (EDC)/N-hydroxysuccinimide (NHS) activation for OBP immobilization, and subsequently constructed a gravimetric sensor for small-molecule detection. Vaish et al. [76] constructed a GPCR immobilization interface using an NTA-functionalized SAM, enabling specific capture and immobilization of His Tagged-GPCRs on a solid surface.

Compared with direct physical adsorption, SAMs provide a more controllable interfacial chemical environment and allow the immobilization mode and level of nonspecific adsorption to be modulated by adjusting the terminal functional groups and surface composition [77]. However, SAMs alone cannot ensure that GPCRs retain their native conformation and function after immobilization. For membrane proteins, appropriate orientation-specific capture strategies or membrane-mimicking environments are also required to help preserve ligand-binding activity [76].

3.3. Covalent Coupling

Covalent coupling immobilizes proteins by forming stable chemical bonds between the protein and the sensor interface and is a commonly used strategy for protein immobilization in biosensors. Compared with physical adsorption, which relies on noncovalent interactions, covalent coupling generally provides greater interfacial stability [78]. EDC/NHS-mediated carboxyl–amine coupling is one of the most widely used approaches. EDC activates surface carboxyl groups and, in the presence of NHS, generates a more stable activated ester, which subsequently reacts with primary amine groups on the protein to form amide bonds, thereby achieving covalent immobilization [79].

Covalent coupling has been applied to OBP sensors and GPCR-related immobilization interfaces. Manai et al. [80] compared two immobilization strategies for porcine OBP on a diamond surface. One involved covalent coupling, whereas the other used His Tag-Ni^{2+}-NTA interactions to achieve relatively controlled orientation, followed by integration into a diamond microcantilever sensor. The two immobilization strategies produced different sensing responses, suggesting that protein orientation may influence the accessibility of binding sites.

For GPCRs, Yuan et al. [81] employed a site-selective covalent immobilization strategy to immobilize the α1A-adrenergic receptor and investigate its ligand-binding behavior, indicating that site-specific covalent attachment can help reduce the effects of random coupling on receptor binding function. Rich et al. [82] used surface plasmon resonance (SPR) to compare direct NTA capture of His Tagged-GPCRs with a “capture-coupling” strategy, in which the receptor was first captured through NTA and subsequently subjected to further covalent coupling using EDC/sulfo-NHS. The results showed that capture-coupling produced a more stable and high-capacity GPCR surface while retaining high receptor activity, indicating that covalent immobilization can improve the retention of GPCRs on sensor chips. Thus, the main advantage of covalent coupling is its enhanced interfacial stability, although its performance still depends on the immobilization site, protein orientation, and accessibility of the active site.

3.4. Biotin–(Strept)avidin Immobilization

Biotin–(strept)avidin immobilization relies on the extremely high noncovalent affinity between biotin and avidin or streptavidin for protein immobilization. The dissociation constant of this interaction is typically in the range of 10^{-14}–10^{-15} M [83,84], resulting in highly stable binding and making this approach widely applicable to the surface immobilization of biomolecules [85].

This strategy has been applied to GPCR-related sensing systems. Hou et al. [86] constructed a multilayer interface on a gold electrode using a mixed SAM and a biotin–(strept)avidin system, and immobilized rhodopsin-containing membrane components through a biotinylated antibody. Electrochemical impedance spectroscopy was subsequently used to characterize the immobilization process. In another study, Hou et al. [87] immobilized ORI7 on a gold electrode modified with a mixed SAM and biotin–avidin system and applied the resulting interface to the electrochemical detection of odorant molecules.

The advantage of biotin–(strept)avidin immobilization lies in its potential for controlling protein orientation. If biotin can be introduced at a predetermined site through site-specific labeling, relatively controlled immobilization orientation may be achieved, potentially improving the accessibility of active sites [85]. However, chemical biotinylation does not necessarily result in oriented immobilization. Lysine-reactive reagents such as NHS-biotin can react with multiple primary amine groups on the protein surface, resulting in biotinylation at different sites and to different extents, which may subsequently lead to heterogeneous spatial orientations upon immobilization [88].

3.5. Metal Chelate Affinity Immobilization

His Tag/NTA metal-chelation immobilization is a tag-mediated affinity immobilization strategy. A His Tag containing several consecutive histidine residues can coordinate with Ni^{2+} and other divalent metal ions chelated by NTA on the surface [89]. A His Tag is typically fused to the N- or C-terminus of a protein through genetic engineering and can therefore reduce, to some extent, the uncertainty in immobilization orientation compared with random amine coupling [89].

This strategy has been directly applied to GPCR- and OBP-related systems. Rich et al. [82] used a Ni^{2+}-NTA surface to directly capture His Tagged-GPCRs, achieving a relatively high receptor surface density while retaining ligand-binding activity; however, the receptors gradually dissociated from the NTA surface over time, resulting in decreased surface stability and activity. Manai et al. [80] used an N-terminal His Tag-Ni^{2+}-NTA interaction to immobilize porcine OBP on a diamond microcantilever surface, achieving relatively controlled protein orientation and a higher sensing response than that obtained with random covalent immobilization.

His Tag/NTA immobilization is generally performed under mild conditions and is reversible. The coordination between His Tag and Ni^{2+}-NTA can be disrupted by imidazole competition or removal of the metal ions, allowing immobilized proteins to be eluted and providing the possibility of surface regeneration [89]. However, the stability of His Tag/NTA coordination is lower than that of covalent bonds, and protein dissociation may therefore occur during long-term detection [82]. In addition, His Tag generally requires the tag to be fused to the N- or C-terminus of the target protein through recombinant expression [89]. Thus, His Tag/NTA provides a relatively mild and controllable immobilization approach for GPCRs and OBPs, but its application still requires consideration of protein orientation, activity retention, and interfacial stability.

3.6. Critical Considerations for GPCR/OBP Immobilization

The applicability of different immobilization strategies depends on the structural and functional characteristics of the recognition elements. For soluble proteins such as OBPs, physical adsorption and covalent coupling can be directly used for surface immobilization, whereas self-assembled monolayers (SAMs) can further modulate the interfacial chemical properties. For GPCRs, whose functions are closely associated with their transmembrane structures and lipid environments, immobilization also requires consideration of receptor orientation, accessibility of ligand-binding sites, and preservation of the membrane environment [83]. The schematic representations of the different immobilization strategies are shown in Figure 2.

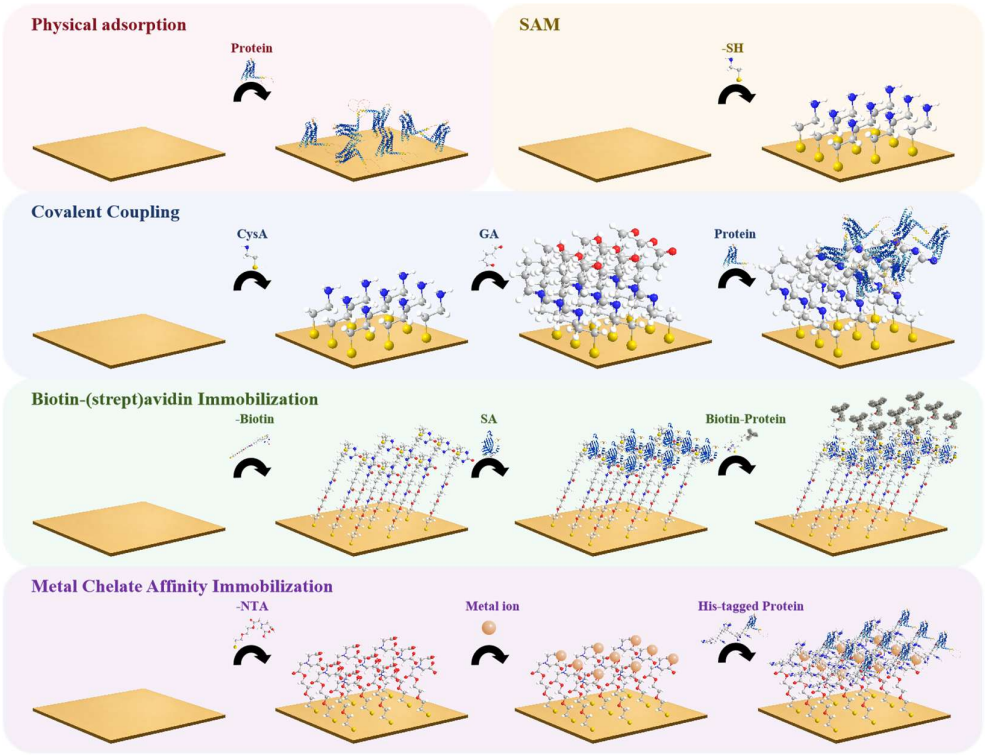


Figure 2. Schematic of immobilization methods for biorecognition elements.

Different immobilization strategies vary in terms of interfacial stability and controllability. Physical adsorption is simple to perform but may suffer from protein desorption and heterogeneous orientation [66–68]. Covalent coupling generally provides greater interfacial stability, although random coupling may compromise the accessibility of ligand-binding sites [66–68]. Biotin–avidin/streptavidin systems and His Tag/NTA interactions enable protein immobilization through specific binding interactions [79,84]; however, the actual orientation still depends on the biotinylation strategy or the position of the affinity tag, while the noncovalent coordination involved in His Tag/NTA immobilization may limit long-term interfacial stability [89]. Importantly, the extent of experimental validation differs among these strategies in GPCR- and OBP-based sensors. Some approaches have been directly demonstrated in GPCR- or OBP-based sensing systems, whereas others are supported mainly by general protein immobilization studies or other biosensing platforms. Their practical applicability to addictive drug detection therefore remains to be further validated. Accordingly, the suitability of an immobilization strategy should be evaluated in the context of the specific recognition element and sensing platform on the basis of experimental evidence.

4. Research Progress of GPCR- and OBP-Based Sensors for Addictive Drug Detection

The interaction of addictive drugs with biological recognition elements can trigger receptor conformational changes, redistribution of local charges, downstream signaling events, or changes in interfacial mass. These molecular events can then be converted into measurable outputs through different signal transduction mechanisms. Accordingly, GPCR- and OBP-based sensing strategies can be broadly classified into four categories: electrical, optical, electrochemical, and acoustic platforms (Figure 3). Depending on the sensor design, these platforms can be used to monitor receptor activation, characterize ligand-receptor interactions, or achieve quantitative drug detection.

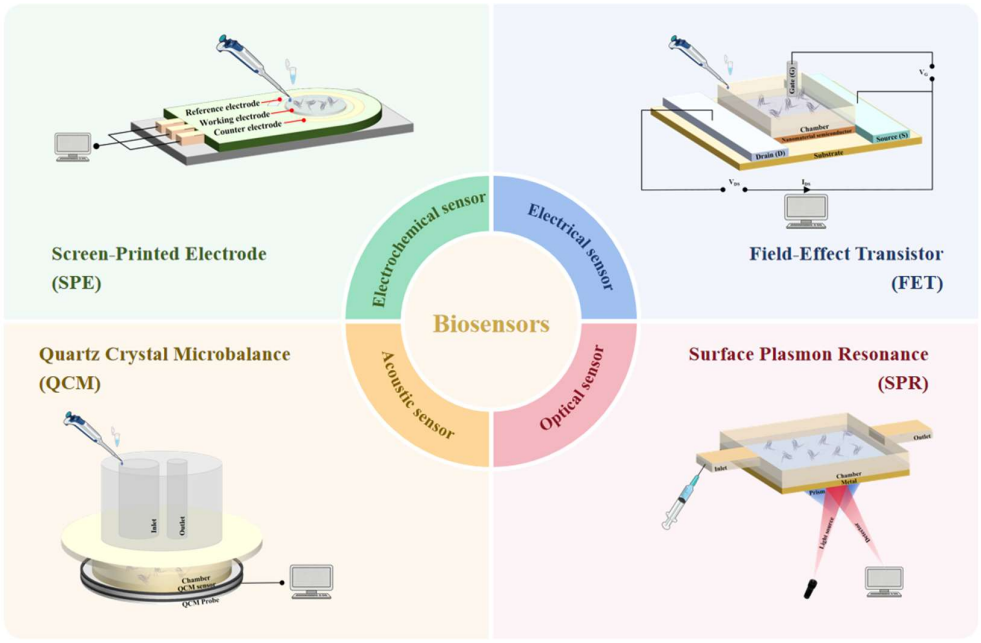


Figure 3. Schematic of biosensors.

From an analytical perspective, the sensing platforms reviewed in this section can be further grouped into three categories according to their targets: (i) direct detection of addictive drug molecules; (ii) monitoring receptor activation induced by drug–receptor interactions; and (iii) detection of endogenous signaling molecules, such as AEA and 2-AG, as a complementary sensing strategy. Although endogenous ligands are not addictive drugs themselves, the receptor-recognition and signal-transduction mechanisms established in these systems may also provide useful frameworks for detecting exogenous cannabinoids.

4.1. Electrical Sensor

Electrical sensing approaches generally monitor changes in cell morphology, adhesion, or interfacial electrical properties following receptor activation and convert these changes into impedance, current, or conductance signals.

Hillger et al. [90] used real-time cell analysis (RTCA) to monitor endogenous CB_2R signaling in lymphoblastoid cell lines (LCLs). Because LCLs are suspension cells, fibronectin was used to mediate their adhesion to the microelectrode surface, allowing changes in cell adhesion and morphology to be recorded as impedance responses. The CB_2R agonist JWH133 produced a concentration-dependent response that was suppressed by AM630 and pertussis toxin, supporting the involvement of CB_2R and $G\alpha_{i/o}$-dependent signaling. This work established RTCA as a label-free means of monitoring GPCR-mediated cellular responses without receptor overexpression.

Thirkettle-Watts et al. [91] applied the same RTCA principle to Chinese hamster ovary (CHO) cells stably expressing μOR and compared their responses to morphine and DAMGO. Although both ligands produced concentration-dependent impedance changes, the response profiles were distinct and included multiple phases. The EC_{50} values for the major impedance peaks were approximately 77.7 nM for morphine and 18.3 nM for DAMGO. Pharmacological inhibition and downstream analyses linked these responses to $G\alpha_{i/o}$- and $G\beta\gamma$-dependent signaling, together with changes involving Protein Kinase B (AKT) and extracellular signal-regulated kinase (ERK) 1/2. Thus, impedance measurements can capture ligand-dependent differences in μOR signaling rather than simply reporting whether the receptor has been activated.

Liu et al. [92] developed a water-soluble μOR to reduce the dependence of receptor sensing on the native membrane environment and incorporated the receptor into a graphene-based electronic sensing platform. Selected hydrophobic residues in the transmembrane region were redesigned, allowing the receptor to remain soluble while retaining ligand-recognition capability. A preliminary Kd of approximately 3.5 nM was reported for morphine. The immobilized receptor was then used to convert ligand interactions into changes in the electronic output of the graphene device. The graphene sensing experiments and the morphine-binding measurements should, however, be considered separately, as the analyte used for the electronic sensing experiment was not necessarily the same as that used for the binding characterization.

Cho et al. [93] reconstituted CB_1R into nanodiscs (NDs) and immobilized the receptor on a single-walled carbon nanotube field-effect transistor (swCNT-FET). Binding of CB_1R to the endocannabinoid AEA and Δ9-THC altered the conductance of the device. AEA produced a concentration-dependent response over 1 fM-10 nM, with an limit of detection (LOD) of 0.11 fM. In serum, a measurable AEA response was observed at concentrations as low as 1 pM. For THC, the linear range was 1 nM-10 μM and the LOD was 0.73 nM. The platform therefore combines receptor-based molecular recognition with direct electronic readout and extends CB_1R-based sensing to cannabinoid analysis in a biological matrix.

4.2. Optical Sensor

Optical platforms use changes in refractive index, fluorescence, or bioluminescence to report drug–receptor interactions or receptor activation. Depending on the sensor design, the measured signal may represent direct binding at the receptor or a downstream functional response.

Bourassa et al. [94] used live-cell SPR to monitor μOR-mediated signaling without fluorescent labeling. HEK-293 cells stably expressing μOR responded to both morphine and DAMGO in a concentration-dependent manner, with signals detectable at approximately 1 nM and more pronounced responses around 100 nM. Pharmacological inhibition indicated contributions from G-protein coupling, ERK1/2 activation, receptor internalization, and other changes in cellular state. The SPR response therefore represents an integrated consequence of μOR activation rather than a direct measurement of ligand binding alone.

Liu et al. [92] also used SPR to characterize ligand interactions with the water-soluble μOR. Immobilized receptor produced concentration-dependent SPR responses, and the preliminary Kd for morphine was approximately 3 nM under the corresponding SPR conditions. This value differs slightly from the approximately 3.5 nM obtained from the related binding characterization, likely reflecting differences in the experimental setup and measurement conditions. The SPR system reduced the requirement for an intact membrane environment and was also used to examine μOR-associated protein interactions, supporting the use of engineered GPCRs as optical recognition elements.

Babazada et al. [95] used an N-terminally truncated human μOR in an SPR assay and incorporated a lipid bilayer to preserve receptor functionality. More than 80% of the immobilized receptor remained functionally active. The measured Kd values for morphine, fentanyl, buprenorphine, methadone, and naloxone were approximately 4.3, 1.7, 1.3, 3.4, and 3.4 nM, respectively, with a strong correlation between Kd and literature inhibition constant (Ki) values (r = 0.93). The assay also provided kinetic information; the dissociation half-lives for buprenorphine and methadone were approximately 58 and 38 s, respectively. These measurements illustrate the ability of SPR to resolve both equilibrium affinity and kinetic properties of opioid–μOR interactions.

Cannaert et al. [37] developed a NanoLuc Binary Technology (NanoBiT) assay based on CB_1R-β-arrestin2 recruitment to characterize the functional activity of synthetic cannabinoid receptor agonists. Across 12 synthetic cannabinoid receptor agonists, EC_{50} values ranged from 2.33 to 5475 nM and E_{max} values from 37% to 378%. MDMB-4en-PINACA, ADB-BINACA, and 4F-MDMB-BINACA were among the most potent compounds, with EC_{50} values of 2.33, 6.36, and 7.39 nM, respectively. Because the readout depends on β-arrestin2 recruitment, this assay is primarily suited to functional profiling and potency ranking rather than direct concentration measurement.

Shaw et al. [96] coupled human CB_2R to a reconstructed yeast signaling pathway and used green fluorescent protein (GFP) expression as the optical output for THC detection. THC produced an approximately linear response from 0.01 to 10 μM (R^2 = 0.98). THCV (a THC analog) activated the system at an initial concentration approximately one order of magnitude lower than THC and produced a maximum response about twice as high. The study illustrates how GPCR signaling can be reconstructed in yeast to generate an optical response, although discrimination among structurally related cannabinoids remains a challenge.

Miettinen et al. [97] developed a multimodal CB_2R-based yeast sensor with fluorescence, colorimetric, and chemiluminescent outputs. In the optimized fluorescent format, CP55940 showed an EC_{50} of approximately 4.64 nM and an LOD of 10 pM, whereas the LODs for THC and JWH-018 were approximately 32 and 1 nM, respectively. The NanoLuc format also reached an LOD of approximately 10 pM for CP55940 and produced a signal-to-noise ratio of up to 687:1. A smartphone camera was sufficient for semi-quantitative readout. The sensor was tested in artificial saliva, urine, and calf serum and was also applied to compound screening, leading to the identification of a plant-derived compound with CB_2R activity. The sample studies, however, were performed mainly with simulated rather than clinical matrices.

Mulvihill et al. [98] developed a CB_1R-based yeast functional sensor by reconstructing the yeast pheromone pathway and incorporating a human $G_{\alpha i3}$-associated signaling component. CB_1R activation was coupled to ZsGreen fluorescence, while N-terminal signal sequences and receptor truncation improved receptor localization. The sterol composition of the host membrane also affected receptor activity. Screening of a compound library containing numerous synthetic cannabinoids identified several compounds with subnanomolar EC_{50} values, including 0.66, 0.01, 1.21, and 0.09 nM for AB-FUBINACA, AB-FUBINACA isomer 1, AB-PINACA, and ADB-PINACA, respectively. Selected compounds were subsequently evaluated in mammalian cells. The results support the use of the yeast system for rapid functional screening while highlighting the influence of the host–cell environment on receptor activity.

Singh et al. [99] developed the genetically encoded fluorescent CB_1R sensor $GRAB_{eCB2.0}$ by inserting circularly permuted green fluorescent protein (cpGFP) into the third intracellular loop (ICL3) of CB_1R. Ligand-induced conformational changes were thereby converted into changes in fluorescence intensity. The sensor responded to 2-AG, AEA, and THC with

EC_{50} values of approximately 85 nM, 815 nM, and 1.6 μM, respectively. The response to 2-AG was comparable to that of native CB_1R, whereas AEA and THC produced weaker responses. This design provides a direct optical readout of CB_1R conformational activation in living cells and is particularly suited to studying endocannabinoid signaling dynamics.

Kroning et al. [100] introduced a single-chain protein-based fluorescent integrator, termed the single-chain protein-based opioid transmission indicator tool (SPOTIT). The system combines μOR or κOR recognition modules with cpGFP and Nb39, converting transient GPCR activation into a persistent fluorescent record. Ligand-induced receptor activation promotes Nb39 recruitment and subsequent cpGFP maturation, allowing previous opioid exposure to be recorded and spatially mapped. Variants included μ-SPOTIT, μ-SPOTIT2, κ-SPOTIT, and a red fluorescent version, while SPOTcal was used to relate sensor output to Ca^{2+} signaling. In mice, μ-SPOTIT2 produced dose-dependent fluorescence following morphine administration: 60 and 100 mg/kg resulted in approximately 3.5-fold and 4.9-fold increases, respectively, whereas 30 mg/kg produced no significant change. Naloxone pretreatment reduced the response. Unlike conventional real-time quantitative sensors, SPOTIT is primarily designed to record the history and spatial distribution of opioid receptor activation.

Shi et al. [101] used SPR to examine the direct binding of CB_1R to 10 synthetic cannabinoid receptor agonists. CB_1R was immobilized on a CM5 chip by amine coupling, and the compounds showed Kd values ranging from 1.571×10^{-6} to 4.346×10^{-5} M. FUB-AKB-48 showed the highest affinity, whereas JWH-018 showed the lowest. Several indazole compounds bound CB_1R more strongly than indole compounds; for example, the Kd values of MDMB-4en-PINACA and AMB-4en-PICA differed by approximately sixfold. By providing direct binding measurements for emerging synthetic cannabinoid receptor agonists, this SPR approach complements functional pharmacological assays and can be used to examine affinity and structure–activity relationships without labeling the analytes.

4.3. Electrochemical Sensor

Electrochemical platforms convert receptor-mediated recognition or downstream ionic events into measurable electrical quantities such as current or potential. Their relatively simple readout makes them attractive for rapid testing and analysis in complex matrices.

Deenin et al. [102] combined CB_2R recognition with lateral-flow separation and differential pulse voltammetry (DPV) for THC detection. THC first formed a complex with an Fc-labeled antibody and was subsequently captured at the CB_2R detection zone, where the redox activity of Fc generated the electrochemical signal. The assay covered a linear range of 0.1–1000 μg/mL and achieved an LOD of approximately 1.30 ng/mL. Responses were also observed for THCA (a THC precursor) and HHC (a semi-synthetic THC analog), whereas CBD, CBN, and CBC produced weaker signals. Measurements of actual cannabis samples agreed well with HPLC results, and the assay required approximately 6 min. This combination of CB_2R recognition and electrochemical readout provides a practical route for rapid cannabinoid analysis in plant-derived materials and finished products.

Kim et al. [103] developed an electrochemical sensor based on CB_1R-derived nanovesicles and receptor-mediated Ca^{2+} signaling. The L341A/A342L mutation altered the G-protein coupling properties of CB_1R and enabled receptor activation to induce Ca^{2+} influx. A carbon-nanotube-printed electrode equipped with a Ca^{2+}-selective membrane converted the resulting ionic change into an open-circuit potential. CP55940 and AEA produced EC_{50} values of approximately 272 and 299 pM, respectively. The sensor also generated an approximately 8 mV response to hemp seed oil containing about 0.001% THC. This design links GPCR activation to an ion-selective electrochemical interface and illustrates a functional route for converting receptor signaling into an electrical output.

4.4. Acoustic Sensor

Acoustic sensing relies on changes in resonant frequency resulting from mass changes at the sensor interface. Among these approaches, QCM is well suited to monitoring protein–small-molecule interactions and volatile compounds.

Cali et al. [75] modified the mosquito odorant-binding protein AgamOBP1 and coupled the engineered OBP to QCM-based sensing for the detection of addictive drug vapors. The S82P mutation increased the binding affinity of AgamOBP1 for THC, cocaine, and MDMA by approximately 13-, 25-, and 105-fold, respectively. D78N and K93H also enhanced binding to cocaine and MDMA, respectively. When immobilized on the QCM surface, the engineered OBP produced frequency changes upon exposure to drug vapors. S82P gave a pronounced response to cocaine vapor, whereas 2-phenylethanol at much higher concentrations produced only a relatively weak signal, indicating some degree of selectivity. Structural analysis suggested that S82P affects the entrance region of the binding pocket and may facilitate ligand access. The sensor retained its performance for at least 10 months, supporting the use of engineered OBPs in QCM-based detection of volatile addictive drugs.

4.5. Summary and Future Perspectives

The analytical performance and functional characteristics of representative GPCR- and OBP-based sensors for addictive drug detection are summarized in Table 3, including the recognition elements, target analytes, transduction mechanisms, key performance metrics, and major advantages and limitations. Because these systems measure different biological or physicochemical events, their performance cannot be compared solely on the basis of the LOD.

GPCR- and OBP-based sensors now encompass electrical, optical, electrochemical, and acoustic modes of signal transduction. Cellular impedance assays and genetically encoded reporters are primarily suited to monitoring receptor activation and pharmacological responses, whereas SPR provides direct measurements of receptor-ligand binding affinity and kinetics. FET and electrochemical platforms have shown greater potential for quantitative analysis, including measurements in complex or practical samples, while OBP-based QCM systems extend biomimetic sensing to volatile drug detection. Accordingly, sensor performance should be evaluated using multiple parameters, including selectivity, functional response, binding affinity and kinetics, detection range, LOD, assay time, matrix compatibility, and stability.

Recognition-element design has also evolved beyond the direct use of native GPCRs and OBPs. Current strategies include reconstruction of the membrane environment, receptor modification, rewiring of intracellular signaling pathways, and engineering of ligand-binding pockets. These approaches enable the recognition properties of GPCRs and OBPs to be coupled to different signal-transduction mechanisms. At the same time, the reported systems differ substantially in their target analytes, signal outputs, and performance metrics. Many functional GPCR sensors were developed primarily for receptor characterization, pharmacological profiling, or drug screening rather than quantitative chemical analysis. Their analytical performance under standardized detection conditions therefore remains to be systematically evaluated. The TAAR family may provide another direction for GPCR-based sensing of addictive drugs.

Table 3. Summary of GPCR- and OBP-based sensors for addictive drug detection.

Year	Recognition Element	Target Analyte	Sensor Platform	Signal Transduction/Readout	Key Performance Metrics	Sample/Application	Major Advantage	Major Limitation
2015	CB_2R in LCLs	JWH133, AM630	RTCA impedance	GPCR activation → changes in cell adhesion/morphology → impedance	JWH133 pEC_{50} 7.82/7.71; AM630 pIC_{50} 6.77/6.85	Endogenous CB_2R signaling in LCLs	Label-free, real-time monitoring of endogenous GPCR signaling	Functional assay; not a direct quantitative drug sensor
2016	μOR-expressing CHO cells	Morphine, DAMGO	RTCA impedance	μOR activation → cellular signaling/morphological changes → impedance	EC_{50}: morphine ~77.7 nM; DAMGO ~18.3 nM for major peaks	GPCR signaling characterization	Distinguishes ligand-dependent signaling profiles	Impedance response reflects integrated cellular events
2019	Water-soluble μOR	Opioid ligands	Graphene-based electronic sensing/SPR	Ligand-μOR interaction → electronic or SPR signal	Morphine Kd ~3–3.5 nM in binding characterization	Ligand binding and μOR–protein interaction studies	Reduces dependence on native membrane environment	Analytical performance of the electronic platform is not fully standardized
2014	μOR-expressing HEK-293 cells	Morphine, DAMGO	Live-cell SPR	μOR activation → G-protein coupling/ERK1/2 activation/internalization → SPR response	Responses detectable at ~1 nM; maximal responses around 100 nM	Live-cell receptor signaling	Label-free monitoring of receptor-mediated signaling	SPR signal represents an integrated cellular response rather than direct binding
2019	Truncated human μOR in lipid bilayer	Morphine, fentanyl, buprenorphine, methadone, naloxone	SPR	Ligand binding → refractive-index change	Kd 1.3–4.3 nM; t1/2: buprenorphine ~58 s, methadone ~38 s	Receptor-opioid binding kinetics	Provides affinity and kinetic information	Requires receptor reconstitution and surface immobilization
2020	CB_1R-β-arrestin2	12 synthetic cannabinoid receptor agonists	NanoBiT	CB_1R activation → β-arrestin2 recruitment → luminescence	EC_{50} 2.33–5475 nM; E_{max} 37–378%	Functional profiling of synthetic cannabinoid receptor agonists	Sensitive functional pharmacological profiling	Not designed for direct concentration quantification
2022	CB_2R in yeast	THC and other cannabinoids	GFP yeast biosensor	CB_2R activation → yeast pheromone pathway → fluorescence	THC: 0.01–10 μM, R^2 = 0.98	Microbial THC production screening	Reconstructs GPCR signaling in yeast	Response depends on cellular signaling context
2022	CB_2R in yeast	CP55940, THC, JWH-018	Fluorescent/colorimetric/NanoLuc yeast biosensor	CB_2R activation → reporter expression	CP55940: EC_{50} 4.64 nM, LOD 10 pM; THC: LOD 32 nM; NanoLuc CP55940; LOD: 10 pM	Simulated saliva, urine, serum; compound screening	Multimodal readout and portable detection	Mainly demonstrated in simulated rather than clinical matrices
2024	CB_1R in humanized yeast	Synthetic cannabinoids	ZsGreen yeast biosensor	CB_1R activation → yeast signaling pathway → fluorescence	EC_{50}: AB-FUBINACA: 0.66 nM; AB-FUBINACA isomer 1: 0.01 nM; AB-PINACA: 1.21 nM; ADB-PINACA: 0.09 nM	Cannabinoid compound screening	Enables functional screening using a human receptor	Host–cell environment influences receptor activity

Table 3. *Cont.*

Year	Recognition Element	Target Analyte	Sensor Platform	Signal Transduction/Readout	Key Performance Metrics	Sample/Application	Major Advantage	Major Limitation
2024	CB_1R-derived $GRAB_{eCB2.0}$	2-AG, AEA, THC	Genetically encoded fluorescent sensor	Ligand-induced CB_1R conformational change → cpGFP fluorescence	EC_{50}: 2-AG 85 nM; AEA: 815 nM; THC: 1.6 µM	Live-cell endocannabinoid imaging	Direct optical monitoring of receptor activation	Primarily designed for biological imaging rather than analytical drug quantification
2024	µOR/κOR-based SPOTIT	Opioids, including morphine	Single-chain fluorescent integrator	GPCR activation → Nb39 recruitment → persistent cpGFP maturation	Morphine: ~3.5-fold and ~4.9-fold fluorescence at 60 and 100 mg/kg, respectively	In vivo opioid exposure mapping in mice	Records previous receptor activation and spatial distribution	Not intended for real-time quantitative concentration measurement
2025	CB_1R	Synthetic cannabinoids	SPR	Direct CB_1R-ligand binding → refractive-index change	Kd 1.571×10^{-6}–4.346×10^{-5} M	Binding affinity analysis of synthetic cannabinoid receptor agonists	Direct, label-free affinity measurement	Affinity values are in the micromolar range; no direct real-sample validation
2024	CB_1R in nanodiscs	AEA, THC	swCNT-FET	Ligand binding → modulation of FET conductance	AEA: 1 fM–10 nM; LOD: 0.11 fM; THC: 1 nM–10 µM, LOD: 0.73 nM	Serum; AEA detectable at 1 pM	Highly sensitive real-time electronic detection	Requires receptor reconstitution and nanodisc/FET integration
2023	CB_2R + anti-THC antibody	THC	Electrochemical lateral-flow assay	THC-antibody complex → CB_2R capture → Fc redox signal	Linear range 0.1–1000 µg/mL; LOD 1.30 ng/mL; ~6 min	Hemp extract; validated against HPLC	Rapid, portable, quantitative electrochemical detection	Uses a combined antibody–receptor recognition scheme
2025	CB_1R-derived cell nanovesicles	CP55940, AEA, THC	CNT-electrodes	CB_1R activation → Ca^{2+} influx → ion-selective potential	EC_{50}: CP55940 ~272 pM; AEA ~299 pM; ~8 mV response to ~0.001% THC	Hemp seed oil	Converts receptor signaling into an electrochemical output	Requires cell-derived receptor nanovesicles and ion-selective interface
2020	Engineered AgamOBP1	Cocaine, THC, MDMA and other drugs	QCM	Drug–OBP binding → interfacial mass change → resonance-frequency shift	S82P affinity improvement: cocaine ~25-fold, THC ~13-fold, MDMA ~105-fold	Drug vapor detection	Extends OBP sensing to volatile drugs; long-term stability	Mainly demonstrated for vapor-phase detection; quantitative analytical performance remains limited

TAAR1 has been shown to recognize or respond to psychostimulants, including methamphetamine, amphetamine, and MDMA, and recent structural studies have provided further insight into the molecular basis of these interactions. However, current TAAR studies have focused mainly on receptor pharmacology, addiction-related mechanisms, and drug–receptor interactions. Mature biomimetic sensing platforms that directly use TAAR as a recognition element for the analytical detection of addictive drugs have yet to be established. TAAR1 and related receptors may therefore provide additional recognition elements for future electrical, optical, or electrochemical sensing platforms.

Mammalian ORs may represent another underexplored class of GPCR recognition elements. Although ORs are primarily associated with odor perception, some mammalian ORs have been reported to interact with drug-related compounds, including codeine, suggesting that their ligand-recognition properties may extend beyond conventional odorants. However, to the best of our knowledge, studies simultaneously combining mammalian ORs, addictive-drug detection, and a sensor transduction platform remain limited or have not yet been reported. This gap suggests that ORs could be explored as alternative molecular recognition elements for biomimetic sensing, particularly when receptor–ligand interactions provide sufficient selectivity for structurally related drug molecules.

5. Conclusions

The rapid emergence of new psychoactive substances has increased the demand for analytical approaches that can provide rapid screening outside conventional laboratory settings. Chromatographic and mass spectrometric methods remain important because they offer high analytical performance and reliable molecular identification, but their dependence on sophisticated instrumentation, trained personnel, and laboratory-based workflows can limit their use for rapid on-site analysis. GPCR- and OBP-based biomimetic sensors provide a complementary strategy by introducing biological molecular recognition into chemical sensing. The studies reviewed here demonstrate that these recognition elements can be coupled with electrical, optical, electrochemical, and acoustic transduction schemes for the detection of addictive drugs and related ligands. Nevertheless, most reported systems remain at the proof-of-concept or early validation stage, and several issues need to be addressed before their analytical performance can be established under practical conditions.

For GPCR-based sensing, maintaining a functional receptor at the sensing interface remains a fundamental consideration. Because GPCR activity depends on the membrane environment, receptor immobilization or reconstitution needs to preserve both ligand accessibility and the conformational properties required for ligand recognition and signaling [95,98]. Membrane-mimetic systems, including lipid-based interfaces, have provided ways to incorporate GPCRs into sensing platforms, but differences in receptor orientation, membrane composition, immobilization conditions, and storage can affect the resulting sensor response [95,98]. These factors make direct comparison between different platforms difficult. OBPs generally offer a simpler route to sensor construction because they are soluble proteins, although their broader ligand-binding profiles can also limit discrimination among structurally related compounds [15]. Thus, characterization of a recognition element should extend beyond its equilibrium binding affinity to include retained activity after immobilization, response reproducibility, and the relationship between molecular binding and the measured sensor output. Previous studies of protein-based sensing also indicate that structural information can be useful for understanding and modifying ligand recognition, but the effects of such modifications ultimately need to be established at the sensor level [65,75].

A more fundamental issue concerns the distinction between pharmacological activity and chemical identity. Activity-based GPCR assays can be advantageous for screening emerging psychoactive compounds because compounds with different chemical structures may still produce a common receptor-mediated response [37,38]. At the same time, receptor activation does not necessarily indicate which specific compound is present. A receptor can recognize multiple ligands, and structurally related compounds may produce overlapping responses. This issue is apparent in cannabinoid receptor-based sensing, where responses have been reported not only for THC but also for THCA and HHC [102]. Such observations indicate that receptor-based sensing may provide information about pharmacological activity without necessarily achieving compound-level identification. This distinction is particularly relevant to forensic and regulatory applications, in which identification of the specific chemical substance may be required. GPCR-based activity sensing is therefore better considered as a functional screening approach that can complement, rather than replace, structure-specific analytical methods.

A similar consideration applies to OBP-based sensing, although the underlying mechanism is different. OBP sensors report ligand-binding events rather than receptor activation, but overlapping binding profiles can still reduce discrimination between chemically related compounds [15,65,75]. Binding affinity or computationally predicted interactions alone are therefore insufficient to establish analytical selectivity. The performance of a recognition element needs to be examined against structurally related compounds, competing ligands, mixtures, and relevant sample matrices. This is also why molecular docking or calculated binding energies should be interpreted primarily as tools for understanding recognition mechanisms rather than as direct predictors of sensor performance [65,75]. Experimental evaluation of response patterns remains necessary to determine whether the molecular recognition observed in solution is retained after incorporation into a sensing platform. Studies of OBP-based sensing have similarly emphasized both the usefulness of structural information and the need to consider the selectivity of the resulting sensing element [15,65].

These observations point toward the value of multiplexed recognition rather than reliance on a single receptor or binding protein. Individual GPCRs or OBPs can interact with several ligands, so a single response may contain insufficient information for unambiguous discrimination. An array of recognition elements with partially overlapping but distinct response profiles could provide a multidimensional pattern and thereby increase the information available for classification. Such an approach is conceptually consistent with the combinatorial nature of biological chemosensory systems and has been explored more broadly in protein-based sensing [15]. However, the usefulness of such arrays depends on experimentally established response patterns rather than on the classification algorithm alone. Performance should therefore be assessed using structurally related compounds, different analyte concentrations, mixtures, and authentic samples, with particular attention to false-positive and false-negative responses and reproducibility across measurements.

The studies summarized in this review also illustrate that the transduction step is as important as molecular recognition itself. Electrical, optical, electrochemical, and acoustic platforms detect different consequences of ligand binding, including changes in charge distribution, receptor conformation, redox behavior, or interfacial mass. Their analytical performance therefore depends not only on the affinity of the recognition element but also on how efficiently the binding event is coupled to the transducer. For example, a high-affinity receptor does not necessarily produce a large or reproducible electrical or optical response if the ligand-induced molecular change is poorly coupled to the sensing interface. Conversely, a measurable sensor response may not directly reflect molecular selectivity if nonspecific interactions contribute substantially to the signal. A useful direction for further development is therefore to establish a clearer relationship between ligand recognition,

receptor or protein state, and the physical signal recorded by the sensor, rather than focusing solely on increasing signal intensity.

Validation in authentic samples represents another step that is still insufficiently addressed in many reported systems. Sensor performance obtained in buffered solutions cannot be assumed to translate directly to biological fluids, plant-derived materials, surface residues, or other complex samples. Matrix effects, endogenous components, sample preparation, nonspecific adsorption, and variation in analyte concentration can all alter the observed response. Accordingly, evaluation with authentic samples and comparison with established analytical methods such as HPLC or chromatographic–mass spectrometric analysis are important for determining whether a biomimetic sensor provides reliable screening information under realistic conditions [97,102].

Taken together, the studies reviewed here suggest that the main value of GPCR- and OBP-based sensing lies not simply in reproducing the analytical functions of conventional chemical methods, but in introducing biologically derived recognition and, in the case of GPCRs, functional pharmacological information into sensing systems. This feature may be particularly useful for screening structurally diverse or newly emerging compounds that are difficult to anticipate in structure-specific assays [37,38]. At the same time, biological activity or ligand binding should not be equated with definitive chemical identification. The future development of these sensors will therefore depend on balancing broad molecular recognition with sufficient discrimination, establishing reproducible recognition-to-signal relationships, and demonstrating performance in complex samples. Combining complementary recognition elements with orthogonal confirmatory methods may provide a more realistic analytical framework for translating GPCR- and OBP-based biomimetic sensing from proof-of-concept studies toward practical drug screening applications.

Author Contributions: L.Z., P.W., B.X. and H.Z. designed the manuscript. L.S.W. and Y.X. wrote the manuscript. L.S.W. and X.Z. completed the drawing of all the figures. X.T., H.G. and H.Z., proofread the article. All authors have read and agreed to the published version of the manuscript.

Funding: This work was supported by the National Key Research and Development Program of China (2024YFB3212300), Key Project of Zhejiang Province (2025C02035), National Natural Science Foundation of China (62120106004), and Fundamental Research Funds for the Central Universities (226-2025-00037).

Institutional Review Board Statement: Not applicable.

Informed Consent Statement: Not applicable.

Data Availability Statement: The original contributions presented in this study are included in the article. Further inquiries can be directed to the corresponding authors.

Acknowledgments: We used AI solely for English language editing and polishing to improve the readability of the manuscript.

Conflicts of Interest: The authors declare no conflicts of interest.

References

1. Kolodny, A.; Courtwright, D.T.; Hwang, C.S.; Kreiner, P.; Eadie, J.L.; Clark, T.W.; Alexander, G.C. The Prescription Opioid and Heroin Crisis: A Public Health Approach to an Epidemic of Addiction. *Annu. Rev. Public Health* **2015**, *36*, 559–574. [CrossRef]
2. Degenhardt, L.; Grebely, J.; Stone, J.; Hickman, M.; Vickerman, P.; Marshall, B.D.L.; Bruneau, J.; Altice, F.L.; Henderson, G.; Rahimi-Movaghar, A.; et al. Global Patterns of Opioid Use and Dependence: Harms to Populations, Interventions, and Future Action. *Lancet* **2019**, *394*, 1560–1579. [CrossRef]
3. Johnson, K.; Pinchuk, I.; Melgar, M.I.E.; Agwogie, M.O.; Salazar Silva, F. The Global Movement towards a Public Health Approach to Substance Use Disorders. *Ann. Med.* **2022**, *54*, 1797–1808. [CrossRef]

4. Mercieca, G.; Odoardi, S.; Cassar, M.; Strano Rossi, S. Rapid and Simple Procedure for the Determination of Cathinones, Amphetamine-like Stimulants and Other New Psychoactive Substances in Blood and Urine by GC–MS. *J. Pharm. Biomed. Anal.* **2018**, *149*, 494–501. [CrossRef]
5. Krotulski, A.J.; Mata, D.C.; Smith, C.R.; Palmquist-Orlando, K.B.; Modell, C.; Vikingsson, S.; Truver, M.T. Advances in Analytical Methodologies for Detecting Novel Psychoactive Substances: A Review. *J. Anal. Toxicol.* **2025**, *49*, 152–169. [CrossRef]
6. Dinis-Oliveira, R.J. Heterogeneous and Homogeneous Immunoassays for Drug Analysis. *Bioanalysis* **2014**, *6*, 2877–2896. [CrossRef]
7. Anzar, N.; Suleman, S.; Singh, Y.; Kumari, S.; Parvez, S.; Pilloton, R.; Narang, J. The Evolution of Illicit-Drug Detection: From Conventional Approaches to Cutting-Edge Immunosensors—A Comprehensive Review. *Biosensors* **2024**, *14*, 477. [CrossRef]
8. Williams, S.F.; Stokes, R.; Tang, P.L.; Blanco-Rodriguez, A.M. Detection & Identification of Hazardous Narcotics and New Psychoactive Substances Using Fourier Transform Infrared Spectroscopy (FTIR). *Anal. Methods* **2023**, *15*, 3225–3232. [CrossRef]
9. Qriouet, Z.; Cherrah, Y.; Sefrioui, H.; Qmichou, Z. Monoclonal Antibodies Application in Lateral Flow Immunochromatographic Assays for Drugs of Abuse Detection. *Molecules* **2021**, *26*, 1058. [CrossRef]
10. Scherer, J.N.; Fiorentin, T.R.; Borille, B.T.; Pasa, G.; Sousa, T.R.V.; von Diemen, L.; Limberger, R.P.; Pechansky, F. Reliability of Point-of-Collection Testing Devices for Drugs of Abuse in Oral Fluid: A Systematic Review and Meta-Analysis. *J. Pharm. Biomed. Anal.* **2017**, *143*, 77–85. [CrossRef]
11. Armenta, S.; Esteve-Turrillas, F.A.; Alcalà, M. Analysis of Hazardous Chemicals by "Stand Alone" Drift Tube Ion Mobility Spectrometry: A Review. *Anal. Methods* **2020**, *12*, 1163–1181. [CrossRef]
12. Zhang, R.; Hu, S.; Ma, C.; Zhang, T.; Li, H. Laser-Induced Breakdown Spectroscopy (LIBS) in Biomedical Analysis. *TrAC Trends Anal. Chem.* **2024**, *181*, 117992. [CrossRef]
13. Bumbrah, G.S.; Sharma, R.M. Raman Spectroscopy—Basic Principle, Instrumentation and Selected Applications for the Characterization of Drugs of Abuse. *Egypt. J. Forensic Sci.* **2016**, *6*, 209–215. [CrossRef]
14. Patel, A.; Peralta-Yahya, P. Olfactory Receptors as an Emerging Chemical Sensing Scaffold. *Biochemistry* **2023**, *62*, 187–195. [CrossRef]
15. Pelosi, P.; Zhu, J.; Knoll, W. Odorant-Binding Proteins as Sensing Elements for Odour Monitoring. *Sensors* **2018**, *18*, 3248. [CrossRef]
16. Sanchez-Reyes, O.B.; Zilberg, G.; McCorvy, J.D.; Wacker, D. Molecular Insights into GPCR Mechanisms for Drugs of Abuse. *J. Biol. Chem.* **2023**, *299*, 105176. [CrossRef]
17. Zhang, M.; Chen, T.; Lu, X.; Lan, X.; Chen, Z.; Lu, S. G Protein-Coupled Receptors (GPCRs): Advances in Structures, Mechanisms and Drug Discovery. *Signal Transduct. Target. Ther.* **2024**, *9*, 88. [CrossRef]
18. Cola, R.B.; Niethammer, S.N.; Rajamannar, P.; Gresch, A.; Bhat, M.A.; Assoumou, K.; Williams, E.T.; Hauck, P.; Hartrampf, N.; Benke, D.; et al. Probing PAC1 Receptor Activation across Species with an Engineered Sensor. *eLife* **2024**, *13*, RP96496. [CrossRef]
19. Yang, D.; Zhou, Q.; Labroska, V.; Qin, S.; Darbalaei, S.; Wu, Y.; Yuliantie, E.; Xie, L.; Tao, H.; Cheng, J.; et al. G Protein-Coupled Receptors: Structure- and Function-Based Drug Discovery. *Signal Transduct. Target. Ther.* **2021**, *6*, 7. [CrossRef]
20. de Bruyne, M.; Baker, T.C. Odor Detection in Insects: Volatile Codes. *J. Chem. Ecol.* **2008**, *34*, 882–897. [CrossRef]
21. Lu, Y.; Liu, Q. Insect Olfactory System Inspired Biosensors for Odorant Detection. *Sens. Diagn.* **2022**, *1*, 1126–1142. [CrossRef]
22. Rihani, K.; Ferveur, J.-F.; Briand, L. The 40-Year Mystery of Insect Odorant-Binding Proteins. *Biomolecules* **2021**, *11*, 509. [CrossRef]
23. Rana, A.; Sharma, D.; Choudhary, K.; Kumari, P.; Ruchika, K.; Yangchan, J.; Kumar, S. Insight into Insect Odorant Binding Proteins: An Alternative Approach for Pest Management. *J. Nat. Pestic. Res.* **2024**, *8*, 100069. [CrossRef]
24. Hutchings, C.J. A Review of Antibody-Based Therapeutics Targeting G Protein-Coupled Receptors: An Update. *Expert Opin. Biol. Ther.* **2020**, *20*, 925–935. [CrossRef]
25. Lorente, J.S.; Sokolov, A.V.; Ferguson, G.; Schiöth, H.B.; Hauser, A.S.; Gloriam, D.E. GPCR Drug Discovery: New Agents, Targets and Indications. *Nat. Rev. Drug Discov.* **2025**, *24*, 458–479. [CrossRef]
26. Garcia-Marcos, M. Heterotrimeric G Protein Signaling without GPCRs: The *Gα-Binding-and-Activating* (GBA) Motif. *J. Biol. Chem.* **2024**, *300*, 105756. [CrossRef]
27. Fisher, I.J.; Lyon, A.M. Q's the Boss: Gαq Regulates Gi-Mediated Calcium Release through PLCβ. *Mol. Cell* **2020**, *80*, 933–934. [CrossRef]
28. Shang, P.; Rong, N.; Jiang, J.-J.; Cheng, J.; Zhang, M.-H.; Kang, D.; Qi, L.; Guo, L.; Yang, G.-M.; Liu, Q.; et al. Structural and Signaling Mechanisms of TAAR1 Enabled Preferential Agonist Design. *Cell* **2023**, *186*, 5347–5362.e24. [CrossRef]
29. Hua, T.; Li, X.; Wu, L.; Iliopoulos-Tsoutsouvas, C.; Wang, Y.; Wu, M.; Shen, L.; Brust, C.A.; Nikas, S.P.; Song, F.; et al. Activation and Signaling Mechanism Revealed by Cannabinoid Receptor-Gi Complex Structures. *Cell* **2020**, *180*, 655–665.e18. [CrossRef]
30. Ibsen, M.S.; Connor, M.; Glass, M. Cannabinoid CB 1 and CB 2 Receptor Signaling and Bias. *Cannabis Cannabinoid Res.* **2017**, *2*, 48–60. [CrossRef]
31. Zhang, Q.; Zhao, Y.; Wu, J.; Zhong, W.; Huang, W.; Pan, Y. The Progress of Small Molecules against Cannabinoid 2 Receptor (CB2R). *Bioorg. Chem.* **2024**, *144*, 107075. [CrossRef]

32. Cravatt, B.F.; Lichtman, A.H. The Endogenous Cannabinoid System and Its Role in Nociceptive Behavior. *J. Neurobiol.* **2004**, *61*, 149–160. [CrossRef]
33. Shao, Z.; Yin, J.; Chapman, K.; Grzemska, M.; Clark, L.; Wang, J.; Rosenbaum, D.M. High-Resolution Crystal Structure of the Human CB1 Cannabinoid Receptor. *Nature* **2016**, *540*, 602–606. [CrossRef]
34. Hua, T.; Vemuri, K.; Pu, M.; Qu, L.; Han, G.W.; Wu, Y.; Zhao, S.; Shui, W.; Li, S.; Korde, A.; et al. Crystal Structure of the Human Cannabinoid Receptor CB1. *Cell* **2016**, *167*, 750–762.e14. [CrossRef]
35. Lichtman, A.H.; Shelton, C.C.; Advani, T.; Cravatt, B.F. Mice Lacking Fatty Acid Amide Hydrolase Exhibit a Cannabinoid Receptor-Mediated Phenotypic Hypoalgesia. *Pain* **2004**, *109*, 319–327. [CrossRef]
36. Munro, S.; Thomas, K.L.; Abu-Shaar, M. Molecular Characterization of a Peripheral Receptor for Cannabinoids. *Nature* **1993**, *365*, 61–65. [CrossRef]
37. Cannaert, A.; Sparkes, E.; Pike, E.; Luo, J.L.; Fang, A.; Kevin, R.C.; Ellison, R.; Gerona, R.; Banister, S.D.; Stove, C.P. Synthesis and in Vitro Cannabinoid Receptor 1 Activity of Recently Detected Synthetic Cannabinoids 4F-MDMB-BICA, 5F-MPP-PICA, MMB-4en-PICA, CUMYL-CBMICA, ADB-BINACA, APP-BINACA, 4F-MDMB-BINACA, MDMB-4en-PINACA, A-CHMINACA, 5F-AB-P7AICA, 5F-MDMB-P7AICA, and 5F-AP7AICA. *ACS Chem. Neurosci.* **2020**, *11*, 4434–4446. [CrossRef]
38. Cannaert, A.; Franz, F.; Auwärter, V.; Stove, C.P. Activity-Based Detection of Consumption of Synthetic Cannabinoids in Authentic Urine Samples Using a Stable Cannabinoid Reporter System. *Anal. Chem.* **2017**, *89*, 9527–9536. [CrossRef]
39. Wang, Y.; Zhuang, Y.; DiBerto, J.F.; Zhou, X.E.; Schmitz, G.P.; Yuan, Q.; Jain, M.K.; Liu, W.; Melcher, K.; Jiang, Y.; et al. Structures of the Entire Human Opioid Receptor Family. *Cell* **2023**, *186*, 413–427.e17. [CrossRef]
40. Wang, D.; Tawfik, V.L.; Corder, G.; Low, S.A.; François, A.; Basbaum, A.I.; Scherrer, G. Functional Divergence of Delta and Mu Opioid Receptor Organization in CNS Pain Circuits. *Neuron* **2018**, *98*, 90–108.e5. [CrossRef]
41. Zhang, Z.; Hu, S.; Geng, S.; Xu, T.; Liu, X.; Lei, Z.; Sun, C.; Sun, H.; Xie, W.; Mu, M. A Multiscale Atlas of Oprm1-Expressing Neurons in the Central Nervous System: Brain-Wide Distribution, Circuit Functions, and Translational Therapeutic Implications. *Neurochem. Int.* **2025**, *188*, 105998. [CrossRef]
42. Lutz, P.-E.; Kieffer, B.L. Opioid Receptors: Distinct Roles in Mood Disorders. *Trends Neurosci.* **2013**, *36*, 195–206. [CrossRef]
43. Ramirez, J.-M.; Burgraff, N.J.; Wei, A.D.; Baertsch, N.A.; Varga, A.G.; Baghdoyan, H.A.; Lydic, R.; Morris, K.F.; Bolser, D.C.; Levitt, E.S. Neuronal Mechanisms Underlying Opioid-Induced Respiratory Depression: Our Current Understanding. *J. Neurophysiol.* **2021**, *125*, 1899–1919. [CrossRef]
44. Lešnik, S.; Bertalan, É.; Bren, U.; Bondar, A.-N. Opioid Receptors and Protonation-Coupled Binding of Opioid Drugs. *Int. J. Mol. Sci.* **2021**, *22*, 13353. [CrossRef]
45. Greenwald, M.K. Effects of Opioid Dependence and Tobacco Use on Ventilatory Response to Progressive Hypercapnia. *Pharmacol. Biochem. Behav.* **2004**, *77*, 39–47. [CrossRef]
46. Zhuang, Y.; Wang, Y.; He, B.; He, X.; Zhou, X.E.; Guo, S.; Rao, Q.; Yang, J.; Liu, J.; Zhou, Q.; et al. Molecular Recognition of Morphine and Fentanyl by the Human μ-Opioid Receptor. *Cell* **2022**, *185*, 4361–4375.e19. [CrossRef]
47. Vaganova, A.N.; Maslennikova, D.D.; Konstantinova, V.V.; Kanov, E.V.; Gainetdinov, R.R. The Expression of Trace Amine-Associated Receptors (TAARs) in Breast Cancer Is Coincident with the Expression of Neuroactive Ligand–Receptor Systems and Depends on Tumor Intrinsic Subtype. *Biomolecules* **2023**, *13*, 1361. [CrossRef]
48. Nair, P.C.; Chalker, J.M.; McKinnon, R.A.; Langmead, C.J.; Gregory, K.J.; Bastiampillai, T. Trace Amine-Associated Receptor 1 (TAAR1): Molecular and Clinical Insights for the Treatment of Schizophrenia and Related Comorbidities. *ACS Pharmacol. Transl. Sci.* **2022**, *5*, 183–188. [CrossRef]
49. Dedic, N.; Dworak, H.; Zeni, C.; Rutigliano, G.; Howes, O.D. Therapeutic Potential of TAAR1 Agonists in Schizophrenia: Evidence from Preclinical Models and Clinical Studies. *Int. J. Mol. Sci.* **2021**, *22*, 13185. [CrossRef]
50. Nair, P.C.; Shajan, B.; Bastiampillai, T. Newly Identified Structures of Trace-Amine Associated Receptor-1 (TAAR1) Will Aid Discovery of next Generation Neuropsychiatric Drugs. *Mol. Psychiatry* **2024**, *29*, 1925–1928. [CrossRef]
51. Liu, H.; Zheng, Y.; Wang, Y.; Wang, Y.; He, X.; Xu, P.; Huang, S.; Yuan, Q.; Zhang, X.; Wang, L.; et al. Recognition of Methamphetamine and Other Amines by Trace Amine Receptor TAAR1. *Nature* **2023**, *624*, 663–671. [CrossRef]
52. Buck, L.; Axel, R. A Novel Multigene Family May Encode Odorant Receptors: A Molecular Basis for Odor Recognition. *Cell* **1991**, *65*, 175–187. [CrossRef]
53. Niimura, Y.; Nei, M. Extensive Gains and Losses of Olfactory Receptor Genes in Mammalian Evolution. *PLoS ONE* **2007**, *2*, e708. [CrossRef]
54. Zhang, X.; Firestein, S. The Olfactory Receptor Gene Superfamily of the Mouse. *Nat. Neurosci.* **2002**, *5*, 124–133. [CrossRef]
55. Young, J.M.; Friedman, C.; Williams, E.M.; Ross, J.A.; Tonnes-Priddy, L.; Trask, B.J. Different Evolutionary Processes Shaped the Mouse and Human Olfactory Receptor Gene Families. *Hum. Mol. Genet.* **2002**, *11*, 535–546. [CrossRef]
56. Young, J.M.; Trask, B.J. The Sense of Smell: Genomics of Vertebrate Odorant Receptors. *Hum. Mol. Genet.* **2002**, *11*, 1153–1160. [CrossRef]

57. Jones, D.T.; Reed, R.R. Golf: An Olfactory Neuron Specific-G Protein Involved in Odorant Signal Transduction. *Science* **1989**, *244*, 790–795. [CrossRef]
58. Cygnar, K.D.; Zhao, H. Phosphodiesterase 1C Is Dispensable for Rapid Response Termination of Olfactory Sensory Neurons. *Nat. Neurosci.* **2009**, *12*, 454–462. [CrossRef]
59. Ho, J.; Perez-Aguilar, J.M.; Gao, L.; Saven, J.G.; Matsunami, H.; Eckenhoff, R.G. Molecular Recognition of Ketamine by a Subset of Olfactory G Protein–Coupled Receptors. *Sci. Signal.* **2015**, *8*, ra33. [CrossRef]
60. Shukla, S.; Nakano-Baker, O.; Godin, D.; MacKenzie, D.; Sarikaya, M. iOBPdb A Database for Experimentally Determined Functional Characterization of Insect Odorant Binding Proteins. *Sci. Data* **2023**, *10*, 295. [CrossRef]
61. Pelosi, P.; Knoll, W. Odorant-Binding Proteins of Mammals. *Biol. Rev.* **2022**, *97*, 20–44. [CrossRef]
62. Pelosi, P.; Iovinella, I.; Zhu, J.; Wang, G.; Dani, F.R. Beyond Chemoreception: Diverse Tasks of Soluble Olfactory Proteins in Insects. *Biol. Rev.* **2018**, *93*, 184–200. [CrossRef]
63. Abendroth, J.A.; Moural, T.W.; Wei, H.; Zhu, F. Roles of Insect Odorant Binding Proteins in Communication and Xenobiotic Adaptation. *Front. Insect Sci.* **2023**, *3*, 1274197. [CrossRef]
64. Leal, W.S. Odorant Reception in Insects: Roles of Receptors, Binding Proteins, and Degrading Enzymes. *Annu. Rev. Entomol.* **2013**, *58*, 373–391. [CrossRef]
65. Langeswaran, K.; Jeyaraman, J.; Mariadasse, R.; Soorangkattan, S. Insights from the Molecular Modeling, Docking Analysis of Illicit Drugs and Bomb Compounds with Honey Bee Odorant Binding Proteins (OBPs). *Bioinformation* **2018**, *14*, 219–231. [CrossRef]
66. Sarcina, L.; Scandurra, C.; Franco, C.D.; Caputo, M.; Catacchio, M.; Bollella, P.; Scamarcio, G.; Macchia, E.; Torsi, L. A Stable Physisorbed Layer of Packed Capture Antibodies for High-Performance Sensing Applications. *J. Mater. Chem. C* **2023**, *11*, 9093–9106. [CrossRef]
67. Rusmini, F.; Zhong, Z.; Feijen, J. Protein Immobilization Strategies for Protein Biochips. *Biomacromolecules* **2007**, *8*, 1775–1789. [CrossRef]
68. Steen Redeker, E.; Ta, D.T.; Cortens, D.; Billen, B.; Guedens, W.; Adriaensens, P. Protein Engineering For Directed Immobilization. *Bioconjug. Chem.* **2013**, *24*, 1761–1777. [CrossRef]
69. Zhao, X.; Ashley, G.M.; Garcia-Gancedo, L.; Jin, H.; Luo, J.; Flewitt, A.J.; Lu, J.R. Protein Functionalized ZnO Thin Film Bulk Acoustic Resonator as an Odorant Biosensor. *Sens. Actuators B Chem.* **2012**, *163*, 242–246. [CrossRef]
70. Du, L.; Wu, C.; Peng, H.; Zou, L.; Zhao, L.; Huang, L.; Wang, P. Piezoelectric Olfactory Receptor Biosensor Prepared by Aptamer-Assisted Immobilization. *Sens. Actuators B Chem.* **2013**, *187*, 481–487. [CrossRef]
71. Singh, M.; Kaur, N.; Comini, E. The Role of Self-Assembled Monolayers in Electronic Devices. *J. Mater. Chem. C* **2020**, *8*, 3938–3955. [CrossRef]
72. Alves, I.D.; Park, C.K.; Hruby, V.J. Plasmon Resonance Methods in GPCR Signaling and Other Membrane Events. *Curr. Protein Pept. Sci.* **2005**, *6*, 293–312. [CrossRef]
73. Sigal, G.B.; Bamdad, C.; Barberis, A.; Strominger, J.; Whitesides, G.M. A Self-Assembled Monolayer for the Binding and Study of Histidine-Tagged Proteins by Surface Plasmon Resonance. *Anal. Chem.* **1996**, *68*, 490–497. [CrossRef]
74. Cali, K.; Tuccori, E.; Persaud, K.C. Gravimetric Biosensors. In *Methods in Enzymology*; Elsevier: Amsterdam, The Netherlands, 2020; Volume 642, pp. 435–468. [CrossRef]
75. Cali, K.; Persaud, K.C. Modification of an Anopheles Gambiae Odorant Binding Protein to Create an Array of Chemical Sensors for Detection of Drugs. *Sci. Rep.* **2020**, *10*, 3890. [CrossRef]
76. Vaish, A.; Silin, V.; Walker, M.L.; Steffens, K.L.; Krueger, S.; Yeliseev, A.A.; Gawrisch, K.; Vanderah, D.J. A Generalized Strategy for Immobilizing Uniformly Oriented Membrane Proteins at Solid Interfaces. *Chem. Commun.* **2013**, *49*, 2685–2687. [CrossRef]
77. Samanta, D.; Sarkar, A. Immobilization of Bio-Macromolecules on Self-Assembled Monolayers: Methods and Sensor Applications. *Chem. Soc. Rev.* **2011**, *40*, 2567–2592. [CrossRef]
78. Camarero, J.A. Recent Developments in the Site-Specific Immobilization of Proteins onto Solid Supports. *Pept. Sci.* **2008**, *90*, 450–458. [CrossRef]
79. Liu, L.; Deng, D.; Xing, Y.; Li, S.; Yuan, B.; Chen, J.; Xia, N. Activity Analysis of the Carbodiimide-Mediated Amine Coupling Reaction on Self-Assembled Monolayers by Cyclic Voltammetry. *Electrochim. Acta* **2013**, *89*, 616–622. [CrossRef]
80. Manai, R.; Scorsone, E.; Rousseau, L.; Ghassemi, F.; Possas Abreu, M.; Lissorgues, G.; Tremillon, N.; Ginisty, H.; Arnault, J.-C.; Tuccori, E.; et al. Grafting Odorant Binding Proteins on Diamond Bio-MEMS. *Biosens. Bioelectron.* **2014**, *60*, 311–317. [CrossRef]
81. Yuan, X.; Shayiranbieke, A.; Xu, R.; Jiang, H.; Yang, Y.; Zhang, Y.; Yin, G.; Zhao, X. Site-Selective Covalently Immobilized Alpha 1A Adrenergic Receptor for Thermodynamic and Extra-Thermodynamic Study of Four Ligands Binding to the Receptor by Chromatographic Methods. *J. Chromatogr. A* **2022**, *1665*, 462827. [CrossRef]
82. Rich, R.L.; Errey, J.; Marshall, F.; Myszka, D.G. Biacore Analysis with Stabilized GPCRs. *Anal. Biochem.* **2011**, *409*, 267–272. [CrossRef]

83. Delgadillo, R.F.; Mueser, T.C.; Zaleta-Rivera, K.; Carnes, K.A.; González-Valdez, J.; Parkhurst, L.J. Detailed Characterization of the Solution Kinetics and Thermodynamics of Biotin, Biocytin and HABA Binding to Avidin and Streptavidin. *PLoS ONE* **2019**, *14*, e0204194. [CrossRef]
84. Sut, T.N.; Park, H.; Koo, D.J.; Yoon, B.K.; Jackman, J.A. Distinct Binding Properties of Neutravidin and Streptavidin Proteins to Biotinylated Supported Lipid Bilayers: Implications for Sensor Functionalization. *Sensors* **2022**, *22*, 5185. [CrossRef]
85. Hanson, E.K.; Whelan, R.J. Combining the Benefits of Biotin–Streptavidin Aptamer Immobilization with the Versatility of Ni-NTA Regeneration Strategies for SPR. *Sensors* **2024**, *24*, 2805. [CrossRef]
86. Hou, Y.; Helali, S.; Zhang, A.; Jaffrezic-Renault, N.; Martelet, C.; Minic, J.; Gorojankina, T.; Persuy, M.-A.; Pajot-Augy, E.; Salesse, R.; et al. Immobilization of Rhodopsin on a Self-Assembled Multilayer and Its Specific Detection by Electrochemical Impedance Spectroscopy. *Biosens. Bioelectron.* **2006**, *21*, 1393–1402. [CrossRef]
87. Hou, Y.; Jaffrezic-Renault, N.; Martelet, C.; Zhang, A.; Minic-Vidic, J.; Gorojankina, T.; Persuy, M.-A.; Pajot-Augy, E.; Salesse, R.; Akimov, V.; et al. A Novel Detection Strategy for Odorant Molecules Based on Controlled Bioengineering of Rat Olfactory Receptor I7. *Biosens. Bioelectron.* **2007**, *22*, 1550–1555. [CrossRef]
88. Kuhn, B.T.; Zimmermann, I.; Egloff, P.; Hürlimann, L.M.; Hutter, C.A.J.; Miscenic, C.; Dawson, R.J.P.; Seeger, M.A.; Geertsma, E.R. Biotinylation of Membrane Proteins for Binder Selections. In *Expression, Purification, and Structural Biology of Membrane Proteins*; Perez, C., Maier, T., Eds.; Springer: New York, NY, USA, 2020; pp. 151–165. ISBN 978-1-0716-0373-4.
89. Zhu, L.; Chang, Y.; Li, Y.; Qiao, M.; Liu, L. Biosensors Based on the Binding Events of Nitrilotriacetic Acid–Metal Complexes. *Biosensors* **2023**, *13*, 507. [CrossRef]
90. Hillger, J.M.; Schoop, J.; Boomsma, D.I.; Eline Slagboom, P.; IJzerman, A.P.; Heitman, L.H. Whole-Cell Biosensor for Label-Free Detection of GPCR-Mediated Drug Responses in Personal Cell Lines. *Biosens. Bioelectron.* **2015**, *74*, 233–242. [CrossRef]
91. Thirkettle-Watts, D. Impedance-Based Analysis of Mu Opioid Receptor Signaling and Underlying Mechanisms. *Biochem. Biophys. Rep.* **2016**, *6*, 32–38. [CrossRef]
92. Liu, R.; Johnson, A.T.C.; Saven, J.G. Water Soluble G-Protein Coupled Receptor Enabled Biosensors. *Transl. Perioper. Pain Med.* **2019**, *6*, 98–103. [CrossRef]
93. Cho, H.; Oh, D.E.; Nam, Y.; Lee, S.H.; Kim, T.H. Bioelectronic Sensing Platform Emulating the Human Endocannabinoid System for Assessing and Modulating of Cannabinoid Activity. *Biosens. Bioelectron.* **2024**, *264*, 116686. [CrossRef]
94. Bourassa, P.; Tudashki, H.B.; Pineyro, G.; Grandbois, M.; Gendron, L. Label-Free Monitoring of μ-Opioid Receptor–Mediated Signaling. *Mol. Pharmacol.* **2014**, *86*, 138–149. [CrossRef]
95. Babazada, H.; Alekberli, T.; Hajieva, P.; Farajov, E. Biosensor-Based Kinetic and Thermodynamic Characterization of Opioids Interaction with Human μ-Opioid Receptor. *Eur. J. Pharm. Sci.* **2019**, *138*, 105017. [CrossRef]
96. Shaw, W.M.; Zhang, Y.; Lu, X.; Khalil, A.S.; Ladds, G.; Luo, X.; Ellis, T. Screening Microbially Produced Δ9-Tetrahydrocannabinol Using a Yeast Biosensor Workflow. *Nat. Commun.* **2022**, *13*, 5509. [CrossRef]
97. Miettinen, K.; Leelahakorn, N.; Almeida, A.; Zhao, Y.; Hansen, L.R.; Nikolajsen, I.E.; Andersen, J.B.; Givskov, M.; Staerk, D.; Bak, S.; et al. A GPCR-Based Yeast Biosensor for Biomedical, Biotechnological, and Point-of-Use Cannabinoid Determination. *Nat. Commun.* **2022**, *13*, 3664. [CrossRef]
98. Mulvihill, C.J.; Lutgens, J.D.; Gollihar, J.D.; Bachanová, P.; Tramont, C.; Marcotte, E.M.; Ellington, A.D.; Gardner, E.C. A Humanized CB1R Yeast Biosensor Enables Facile Screening of Cannabinoid Compounds. *Int. J. Mol. Sci.* **2024**, *25*, 6060. [CrossRef]
99. Singh, S.; Sarroza, D.; English, A.; McGrory, M.; Dong, A.; Zweifel, L.; Land, B.B.; Li, Y.; Bruchas, M.R.; Stella, N. Pharmacological Characterization of the Endocannabinoid Sensor $GRAB_{eCB2.0}$. *Cannabis Cannabinoid Res.* **2024**, *9*, 1250–1266. [CrossRef]
100. Kroning, K.; Gannot, N.; Li, X.; Putansu, A.; Zhou, G.; Sescil, J.; Shen, J.; Wilson, A.; Fiel, H.; Li, P.; et al. Single-Chain Fluorescent Integrators for Mapping G-Protein-Coupled Receptor Agonists. *Proc. Natl. Acad. Sci. USA* **2024**, *121*, e2307090121. [CrossRef]
101. Shi, X.; Kuai, L.; Xu, D.; Qiao, Y.; Chen, Y.; Di, B.; Xu, P. Surface Plasmon Resonance (SPR) for the Binding Kinetics Analysis of Synthetic Cannabinoids: Advancing CB1 Receptor Interaction Studies. *Int. J. Mol. Sci.* **2025**, *26*, 3692. [CrossRef]
102. Deenin, W.; Wenninger, N.; Schmid, M.G.; Kalcher, K.; Ortner, A.; Chaiyo, S. Rapid Electrochemical Lateral Flow Device for the Detection of Δ9-Tetrahydrocannabinol. *Anal. Chim. Acta* **2023**, *1279*, 341768. [CrossRef]
103. Kim, M.; Kim, H.; Lee, S.; Lim, I.; Kim, E.; Oh, U.; Jang, Y. Ultra-Sensitive Biosensor Based on Cell-Derived Nanovesicles for CB1 Receptor-Targeted Drug Development in a Live Cell-Free Platform. *Anal. Chem.* **2025**, *97*, 9284–9290. [CrossRef]

Disclaimer/Publisher's Note: The statements, opinions and data contained in all publications are solely those of the individual author(s) and contributor(s) and not of MDPI and/or the editor(s). MDPI and/or the editor(s) disclaim responsibility for any injury to people or property resulting from any ideas, methods, instructions or products referred to in the content.